

LUT UNIVERSITY  
LUT School of Energy systems  
LUT Mechanical engineering

*Harri Koivumaa*

**Influence of material selection on gearwheel strength calculation accuracy**

30.11.2021

Examiners: Professor Jussi Söpanen  
D. Sc. (Tech.) Charles Nutakor

## TIIVISTELMÄ

LUT-Yliopisto  
LUT School of Energy systems  
LUT Konetekniikka

Harri Koivumaa

### **Materiaalivalinnan vaikutus hammaspyörien lujuuslaskennan tarkkuuteen**

Diplomityö

2021

71 sivua, 28 kuvaa, 6 taulukkoa ja 4 liitettä

Tarkastajat: Professor Jussi Sopenen  
D. Sc. (Tech.) Charles Nutakor

Avainsanat: Hammaspyörän materiaali, lieriöhammaspyörä, Hammaspyörän lujuuslaskenta

Opinnäytetyö on kaksiosainen. Tämän opinnäytetyön tavoitteena oli tutkia kuinka hiiletyskarkaisuteräksen laadun valinta vaikuttaa hammaspyöräparin lujuuden laskennan tarkkuuteen, sekä suunnitella tarvittavat muutokset testipenkkiin suunniteltujen hammaspyörien testausta varten. Parhaan teräslaadun valinta on kriittinen vaihe ja hammaspyörien lujuuslaskennan tarkkuudella on valtava merkitys lopulliseen laatuun.

Hammaspyörien lujuuslaskenta suoritettiin KISSsys ohjelmistoa hyödyntäen. Laskelman perusteena käytettiin SFS-ISO 6336 standardia. Pohjana käytettiin olemassa olevan ja testatun vaihteen mallia, johon laskettiin uudelleen yksi hammaspyöräpari noin 10 tunnin laskennalliselle kestoaikalle. Varsinainen testaus suoritetaan opinnäytetyön ulkopuolella, tarvittavat laitteet suunnitellaan opinnäytetyön yhteydessä.

Vertailu eri hiiletyskarkaisuteräksillä suoritettujen lujuuslaskujen välillä tehtiin geometrisesti identtisillä hammaspyörillä. Lopulliset testauksessa käytettävät hammaspyörät eroavat toisistaan hampaan leveyden osalta. Testipenkki suunniteltiin modulaariseksi, jotta myös olemassa olevia kiinnittimiä voidaan käyttää.

Aiemmat laskelmat KISSsys ohjelmistossa antavat viitteitä, että laskenta ei ota kaikkia tarvittavia muuttujia huomioon. Vaikuttaisi siltä, että materiaalin murtolujuus olisi vaikuttava tekijä eikä karkenevuus vaikuttaisi lopputuloksiin. Opinnäytetyössä suunnitellut hammaspyörät sekä testipenkit muutokset mahdollistavat käytännön testauksen. Hammaspyörien lujuuslaskenta tehtiin rajoitetulle käyttöajalle, jotta täyden käyttöajan testaus voidaan tehdä järkevän ajan puitteissa.

## **ABSTRACT**

LUT University  
LUT School of Energy systems  
LUT Mechanical engineering

Harri Koivumaa

### **Influence of material selection on gearwheel strength calculation accuracy**

Master's thesis

2021

71 Pages, 28 Figures, 6 Tables and 4 Appendices

Examiners: Professor Jussi Sopenen  
D. Sc. (Tech.) Charles Nutakor

Keywords: Gearwheel material, spur gear, gear strength calculation

The thesis has two parts. Gear strength calculation to limited lifetime with different case carburizing steels and design changes to existing testbench to test gearwheels. Selecting the best steel for gearwheels is critical and calculation accuracy has a large impact on the achieved quality.

Gear strength calculations were made with KISSsys software, which is based on the standard SFS-ISO 6336. The existing and tested gearbox model was used as starting point where one gearwheel pair was redesigned for a limited lifetime, approximately 10h. Physical tests are performed outside the thesis and suitable equipment is designed in the thesis.

Comparison between gear strength calculation with different case carburizing steel was made with identical geometry. The final design of gearwheels for full lifetime tests was made by adjusting face width to achieve desired calculated lifetime. Testbench design was made modular for using existing fixtures.

Previous calculations indicate that KISSsys gear strength calculation does not necessarily consider all variables. It seemed that results are dependent on material tensile strength and hardenability does not affect calculation results. New calculated gearwheels and testbench design made it possible to test the theory in practice. Gear strength was calculated to limited lifetime to make full lifetime tests possible in a reasonable time.

## **ACKNOWLEDGEMENTS**

I am more than grateful to my wife and my son who had supported me during all the hard times during my journey to this point. Reconciling of my family, study and work was not always easy for them.

Special thanks go to Charles Nutakor who did much more than minimum to help me with writing thesis. Motivating and helping also in weekends and after work hours was not necessary for him but it made possible to finish thesis in time. Jussi Sopenen was also supporting and always tried to find solutions for occurring problems and delays. Knowledge and competence of Jussi and Charles made a big impression to me.

I also want to thank Tero Tuomela who was thesis supervisor at Katsa. He did a good job to help me with thesis project.

Finally, I want to thank all my friends and colleagues who have supported me during my thesis and studies. You know who you are so pat yourself on the back. Kiitos.

Harri Koivumaa

Kangasala 30.11.2021

## LIST OF SYMBOLS AND ABBREVIATIONS

BTP	Total load in the plane of action
DAMA	Design, Analyze, Manufacture and Assess
DIN	Deutsche Industrie Normen
DNV	Det Norske Veritas
FEM	Finite Element Method
ISO	International Organization for Standardization
N	Nitrogen
Nb	Niobi
PTO	Power Take Off
QT	Quenched and Tempered
RG	Running gears
RPM	Revolution Per Minute
SFS	Finnish Standards Association
STBG	Single Tooth Bending Fatigue
Ti	Titanium
$\alpha_n$	pressure angle
$\alpha_{KP}$	profile angle of the chamfer involute
$\alpha_{prP}$	protuberance angle
$\beta$	helix angle
$b$	face width
$C_{\gamma a}$	mean value of mesh stiffness per unit face width
$h_{aP}$	addendum
$h_{FaP}$	tip form hight
$h_{fP}$	dedendum
$h_{prP}$	protuberance height
$J_{1,2}$	moment of inertia per unit face width
$m_{1,2}$	is relative individual pinion gear mass per unit face width referenced to line of action
$m_{red}$	the relative mass of a gear pair

$n_1$	Rotation speed inRPM
$\rho_{fP}$	root radius
$p$	length of path of contact
$pr$	Remaining protuberance after grinding
$q$	circular pitch
$r_b$	the base radius
$u$	the gear ratio
$v$	circumferential velocity
$Z$	the number of teeth of gearwheel

## TABLE OF CONTENT

### TIIVISTELMÄ

### ABSTRACT

### ACKNOWLEDGEMENT

### LIST OF SYMBOLS AND ABBREVIATIONS

## TABLE OF CONTENT

<b>1</b>	<b>Introduction.....</b>	<b>9</b>
1.1	Background and motivation.....	9
1.2	Literature review.....	11
1.3	Scope and objectives.....	16
1.4	Research questions and hypothesis.....	17
<b>2</b>	<b>Gear calculation methods and theory .....</b>	<b>18</b>
2.1	Material selection.....	18
2.1.1	18CrNiMo7-6.....	18
2.1.2	20MnCr5.....	19
2.1.3	20NiCrMo2-2.....	20
2.2	Basic gearwheel calculations .....	21
2.3	Gearwheel strength calculation.....	22
2.3.1	Application factor $K_A$ .....	24
2.3.2	Internal dynamic factor $K_V$ .....	24
2.3.3	Face load factors $K_H\beta$ and $K_F\beta$ .....	29
2.4	Keyway strength calculation.....	35
2.5	Gearwheel manufacturing.....	36

2.5.1	Hobbing .....	36
2.5.2	Heat treatment.....	37
2.5.3	Gear grinding .....	38
2.6	Expected damage mechanisms .....	39
2.6.1	Pitting.....	39
2.6.2	Scuffing.....	41
<b>3</b>	<b>Results and discussion .....</b>	<b>45</b>
3.1	Gearwheel design specifications.....	45
3.2	Gearwheel calculation process.....	48
3.3	Results of gear strength calculation .....	49
3.4	Gearwheel manufacturing.....	54
3.5	Dynamic test bench design specifications .....	57
3.6	Results of test bench design.....	59
<b>4</b>	<b>Conclusion .....</b>	<b>62</b>
4.1	Future studies .....	63
	<b>REFERENCES.....</b>	<b>64</b>
	<b>APPENDICES</b>	
	Appendix I: Drawing of gearwheel one 18CrNiMo7-6	
	Appendix II: Drawing of gearwheel two 18CrNiMo7-6	
	Appendix III: Drawing of gearwheel one 20MnCr5	
	Appendix IV: Drawing of gearwheel two 20MnCr5	



# 1 INTRODUCTION

Scope, reason and limitations of the thesis is presented in this section. Also existing studies are introduced as reference and to give understanding of the nature of the thesis.

## 1.1 Background and motivation

Gearwheels are one of the most common ways to transfer power from the power source to the desired location in many transmissions or drivetrain systems. Gear transmission also makes it possible to adjust speed and torque as needed. Gearboxes are divided into drives with a constant transmission ratio and drive with a variable transmission ratio (Jelaska 2012, p. 3). Gears may come in various forms and types. Gears are used widely in different applications. Marine, mobile, and vehicles use gears and gearboxes to transfer power from the motor to make moving possible. Also, Power Take-Off (PTO) gearboxes are used to use motor-produced power in different applications. A typical application is PTO for hydraulic pumps. Industry uses gear actuators for different tasks. Adjusting and lifting, for example, use typically worm gear systems due to good accuracy. Also producing electricity typically needs gears in some phase. (Katsa 2021.) Wind turbines have a gearbox to convert the low rotating speed of the rotor to a speed suitable for generators, although direct drive units are becoming more common (Semken 2015, p. 711).

Gear pumps form another kind of method of power transfer that employs the meshing of gears. Typical use of gear pump is when the viscosity of the liquid is too high (Borremans 2019, p. 71). Most of the gears in these applications operate under varying and sometimes harsh operating conditions. To withstand the demanding loads and dynamics in these applications gears are designed to achieve adequate fatigue strength, resist wear, and possess a tough core to prevent brittle failure under loaded conditions. As such, accurate strength calculations are important to ensure a longer lifetime (service life) of the gearbox. Cyclic gear tooth loads result in various forms of gear material fatigue. Considering that the gear tooth is a cantilevered structure (Figure 1) excessive gear tooth forces cause it to bend, creating high stresses that lead to gear tooth breakage. However, too strong gears unnecessarily increase weight and add costs. In some cases, also third-party classification

demands strength calculation made in a specific way to achieve needed reliability. (DNV 2021, p. 42.)

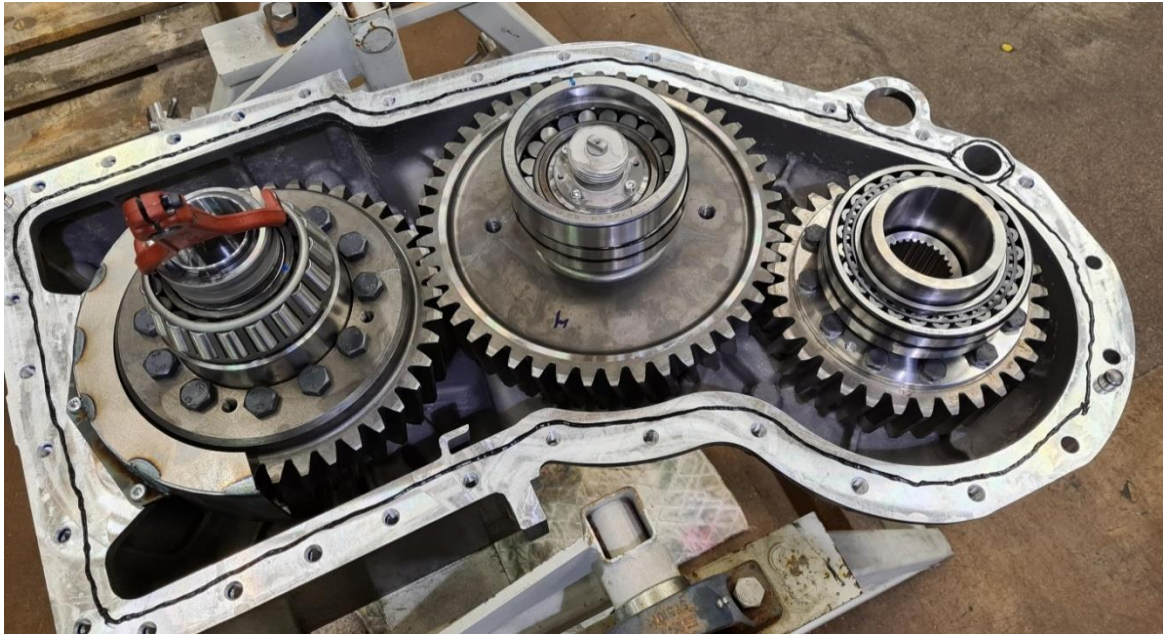


**Figure 1.** Opened gearbox showing helical gears, shafts, and bearings

Gearwheels are typically made from steel although very recently the dynamics of additive manufactured plastic gears are being studied for their suitability in applicable systems (Dennig et al. 2021, p. 1). Most demanding gearwheels are typically case carburized allowing the finished gearwheel surface to be improved. Case carburizing makes the gearwheel surface extremely hard with improved wear resisting properties (Hippenstiel 2007, p. 1). The core of the gear tooth remains softer and makes it resilient to bending (Ramasamy et al. 2020, p. 3). Gearwheel size has a significant impact on the case hardening process and should be considered when choosing the gear material. Gearwheels with large teeth have such a large mass that the hardening process does not affect the tooth at all. Small teeth and steel with too good hardenability can lead to through hardening and brittle teeth. Different steel alloys must be used to avoid these extremes.

Case hardening is not the only option for gearwheel surface hardening. Induction hardening or coating, for example, nitriding, is also a possibility. Induction hardening usually costs less and the process is faster in small batches. A nitride surface gives also good protection for

corrosion. Steel grades used in gearwheels are typically made for Quenching and Tempering (QT) with carbon levels 0.25-0.60%. These steels are suitable for direct hardenings such as nitriding or induction hardening. The common steel used in gearwheel with direct hardening is 42CrMo4. Steel grades used in case carburizing are QT steels, but carbon level is lower, 0.1-0.3%. Surface hardening demands a carbon-rich atmosphere during heating. The typical steel grade used in the gear industry in Finland is 18CrNiMo7-6 (Kivivuori 2016, p. 13).

A better understanding of how material selection affects gearwheel strength calculation allows adjusting calculation parameters to meet reality. With more accurate gearwheel strength calculation, it is possible to produce lighter and strong enough gearboxes for more demanding customers. Not only does this help product development but also component sales area. Component customers do not always have any knowledge of gearwheel design and drawings can be decades-old or made from different continents. In these cases, a well-reasoned suggestion of material change could benefit all parties involved. When the strength calculation method is confirmed, it is possible to make reasonable fast calculations to ensure that material change does not weaken gearwheel power transmitting abilities. Choosing the best possible material is not just finding the cheapest solution, but also finding the best compromise for the price, delivery time, and other material-specific properties. It is known that materials behave differently in the hardening process. In some cases, shape distortion in the hardening process causes significant costs or even failed workpieces. More accurate gear strength calculation could make it possible to change material based on these other demands and reduce manufacturing costs and delivery times.

## 1.2 Literature review

Steel alloys used in gearwheels are preferred differently in different market sectors. Western Europe prefers 20MnCr5 and 18CrNiMo7-6 due to historical reasons. Steel compositions are chosen to achieve high performance requirements for gear components. (Tobie et al. 2017, p. 2.) studied how these steel grades could be improved by modification of standard alloy. The reason for needing different alloys is stress behavior in tooth structure. Increasing transmitted torque typically means increased tooth size. When gear size increases, load-induced stress becomes larger. This leads to the need for a larger hardening depth. Hardening depth is possible to control with the case carburizing process but it has limitations. Material

hardenability is a key factor to achieve desired results. Changing material properties by microalloying or a more radical change of composition may have also other impacts that must be taken into consideration.

Tests must be made to ensure that calculations are accurate enough to rely on. Another major aspect to improve existing alloys is the possibility to influence quench distortions. Adding Niobium (Nb), Titanium (Ti), and Nitrogen (N) to 25MoCr4 resulted in approximately 50% reduced deviation in roundness. The study suggests that increased costs for alloying are compensated by saved time in straightening and hard machining costs. Another cost and time reduction possibility lies in reduced heat treatment time. Alloyed material is possible to carburize at higher temperatures and achieve 25 to 40 percent time save (Tobie et al. 2017, p. 11). Two main reasons to be unable to higher temperature hardening are grain size growth in steel and lack of heat treatment plants capable of over 950°C hardening temperatures (Hippenstiel 2007, p. 2). Testing gear tooth bending stress has two major types of methods. Running Gears (RG) and Single Tooth Bending Fatigue (STBF). STBF testing is simple and has fewer uncertainties. However, this may have too high a result. Root stress is not entirely similar compared to the RG test. Some correction coefficient is needed when translating test results to real-life scenarios. (Concli et al. 2021a, p. 6.) used Finite element method (FEM) calculations to theoretically find the right correction coefficient. Different fatigue criteria give significantly different results.

The accuracy and value of the calculated correction factor differs also between varied materials. The main conclusion of the paper was that choosing the right fatigue criteria for translation is not straightforward. The choice should be made by considering the material. Since the RG test is significantly easier to make, it would be beneficial to calculate and confirm the right correction coefficient for used materials. Concli et al. (2021a, p 11.) found out that typically used fixed correction coefficient value 0.9 is on the safe side in calculations. In most cases in the study, the value was above 0.9 and thus material performance was underestimated. However, there were some cases where the value of the correction coefficient was below 0.9 and which resulted in safety issues. Maláková et al. (2019, p. 8) showed that even when calculations are accurate and suitable material is found, several variables may affect the actual lifespan of gears. For example, the way of lubrication

is supposed to be optimal. If gearbox design is flawed in this way, lifespan may be shorter than expected.

The geometry of tooth root area is not specified exactly in standards (ISO 53 2020, p. 16). Exact geometry of the tool used to manufacture teeth is not always known to designer. Root geometry and grinding allowances may be different in different factories. The reason for this is different hardening processes and company practices. Same gearwheel purchased from different subcontractors could have slightly different tooth root geometry. Since calculations and used factors are case-specific and are typically a good amount on the safe side, there is a need to verify these in actual tests. Full lifetime tests are impossible to conduct with a normal gearbox since lifetime is calculated remarkably high and test period would be extremely long. Gearboxes in production are tested with different procedures agreed on with customers and they prove that product lifetime is acceptable. There is no proofing if strength is just enough or if a structure is too strong. Additional strength causes extra weight and adds costs. Test with calculations made in a limited lifetime makes it possible to test if the maximum lifetime calculated is correct.

Computer-aided gear design has made it possible to model gears and complex systems more precisely and in detail. Goldfarb et al. (2020, p. 73) introduced fundamental steps in software-based gearwheel design. DAMA (Design, Analyze, Manufacture and Assess) model includes calculation of gearwheels, manufacturing, and finally testing how theory happened in practice. Since manufacturing factories and used tools affect the result, calculation accuracy should be ensured in critical cases or cost reduction projects. Reverse engineering is possible, meaning that if deviations are noted, calculations can be corrected to correspond to test results. Gear tooth failures can occur for several reasons. The tooth root area is most vulnerable to breakage due to bending fatigue. The strength of tooth root is the combination of several factors. Material cleanliness, case depth and hardness, shape and roughness of tooth root, and residual stresses affect final strength (Gasparini et al. 2009, p. 1). Standard SFS-ISO 6336-3 provides methods to calculate safety factors against bending fatigue. It is noticeable that given equations do not apply if the permissible number of cycles are less than  $10^3$ . Under that range, the elastic limit of gear tooth may be exceeded, and

plastic yielding damage is possible. Gear tooth bending or surface compressive stress is possible when the elastic limit is exceeded (SFS-ISO 6336-1 2020, p. 18).

Flank failures are divided into pitting and scuffing failures. In terms of gear scuffing failures, miscalculating gear strength, or neglecting the fundamentals of gear friction could cause scuffing failures. The reason behind this phenomenon is excessive heat generation and gear tooth contact fatigue lives (Dennig et al. 2021, p. 2). These are also associated with failure modes such as spalling and micro-pitting (Vullo 2020b, p. 544). Combined sliding and rolling motions of the gear tooth interface cause gear contact friction in lubricated gears, which leads to friction losses and reduced service life of gears and bearings (Nutakor et al. 2017, p. 43; Guillermo et al. 2019, p. 350; Rycerz et al. 2019, p. 2).

Lubrication at the gear tooth varies from full film to elastohydrodynamic lubrication (EHL) or boundary lubrication conditions (Nutakor et al. 2019, p. 510). EHL occurs in lubricated, non-conformal contacts and where mating surface deformation affects the thickness of lubrication film (Björling et al. 2013, p. 19; Hansen et al. 2020, p. 1). Gear tooth surface, operating condition, and lubricant characteristics are dictated by lubrication conditions at the EHL contact (Nutakor et al. 2019, p.511). Pitting (used in place of macropitting) is caused by alternating contact stresses of the gear flank. The tolerated size and number of pits are dependent on the field of the application as indicated in (SFS-ISO 6336-2 2020, p. 12). A similar phenomenon is micropitting which has some unique character and should be taken into consideration separately (Vullo 2020b, p. 439).

Contact stresses can be reduced in strength calculation in several ways. A larger surface contact area reduces stress, and this is achieved by extending the width of the tooth. Stresses can be managed also by changing helix angle or pressure angle. Helix and pressure angle change alters the direction of force to gear flank and thus helps to reduce surface stress. These modifications cause side effects and may prompt other challenges. Helix angle adds loads to bearings and is particularly difficult in cases where the direction of rotation is changing. Pressure angle changes could cause additional tooling costs in production when using hobbing tools or similar where the shape of the tool defines the finished profile. Scuffing failures are not dependent only on calculation but also on the implementation of

lubrication in a gearbox. If lubrication is not as effective as calculation presumes, scuffing could occur despite correct calculations. Since gear flank surface hardness has a major impact on damage resistance, material selection is important. Selecting the wrong material could lead to a soft flank surface. Material selection also has an impact on gear deformation during the hardening process. Alloying influences hardenability and alters stresses formed in the quenching phase of the hardening process. These stresses cause deformations. Large deformations could lead to situations where ground tooth flanks have different hardening depths or some teeth may lose desired hard surface.

The first task to avoid these failures in the design phase is choosing the right material. The size of the tooth has a major impact on final strength. Gear steel strength in an optimal situation is insignificant if those conditions are impossible to achieve. Gearwheel physical size is often limited by external demands, also too big gears mean too heavy and expensive. Gearwheel strength calculation is an iterative process where the starting point is the best estimate for suitable material. The calculation may progress to a situation when the originally selected material is no more suitable. Often this is something that calculation does not show but could be interpreted from the jominy curve. In a typical case, also the material selection is limited by default for several reasons. Raw material for gearwheels is most cost-effective when purchasing in larger quantities. This results in a situation where the amount of different materials is appropriate to keep as low as possible. Also, the availability of gear steels is different around the world. Calculations may need several iterations from material selection to rough and fine sizing modifications stage of the gear.

Modern calculation programs make the process quite fast since the beginning of the iteration process is made with light calculation needs. Typically calculations become demanding after shafts, bearings, and forces from them are captured in the calculations. Flank strength depends on other factors such as lubricant type and lubricant base oil and additives. Lubrication oil and method to circulate oil is possible to add into calculations. The operating environment may affect oil so it is mandatory to know if the machine is to be used in a cold or hot environment. Since final usage varies greatly, the needed calculated safety factors vary. In most cases, it is needed to presume some degree of misuse and overload. Also, maintenance possibilities may cause the need to add more safety factors. For example, ships

are in big trouble if the gearbox breaks down in the middle of the sea. It could be a life-threatening situation so safety factors are significantly larger than less critical applications. Mobile applications and vehicle gearbox needs are particularly difficult to estimate. Forces in these applications are typically not extremely large but could reach extremes in some situations. For example, car tires could easily get stuck in off-road driving and cause enormous torque peaks.

### 1.3 Scope and objectives

Designing a new gearbox ends with always testing the finished product. Since gearboxes are designed for very long service life, it is not possible to make full lifetime tests. The test process is determined with the client to show any flaws in design and ensure that power transmitting ability is as demanded. Experience has shown that the lifetime of gearboxes is typically much longer than calculated. Large safety factors were used in the past since gear strength calculations were not as accurate as today. These old habits may cause these calculations to be too careful and do not necessarily correspond to the situation today. Even if it is better to be safe side, it could result in unnecessarily massive and expensive products. Existing literature does not explain how material change affects gearwheel strength calculation accuracy. The purpose of this thesis is to fill this research gap by calculating gear strengths for different case carburizing steels to achieve a limited lifetime in a gearbox and design a test plan for a full lifetime test for calculated gears. The thesis includes also designing the necessary modifications for existing test equipment. Objectives of the thesis are as follows:

- Study possible causes of gear strength calculation inaccuracies when using case carburizing steel.
- Designing and making strength calculations for a spur gear pair with different case carburizing steels.
- Redesign existing test equipment to be suitable to perform full lifetime tests.
- Design a test procedure to allow limited lifetime tests to be performed.

Due to constraints with the test bench construction, the final results from full lifetime tests are not included in the thesis. The test gearbox is designed to use spur gears to avoid



unnecessary variables like axial forces to bearings. Low axial forces from gearwheels also made possible to work with low compression fitting. Gearwheel fitting to shaft is made with key and just minor compression fit to centralize gears. This is to ease the dismantling and assembly process since just one gearbox is used. All other components are kept the same or changed to similar if broken during a test. The lubrication and test environment are kept similar in all tests. All tested gearwheels have the same accuracy grade and same quality finish. The lifetime of gearwheels between different materials is adjusted by the width of the tooth. Otherwise, the design is the same in all tested gearwheels.

#### 1.4 Research questions and hypothesis

Effect of the material to strength calculation and manufacturing is not studied enough and deeper understanding is needed to increase competitiveness. As such, this thesis seeks to find answers to

- Are calculated and found strength differences the same with every used material?
- What is the most simple way to determine the best suitable material?
- Can calculation accuracy be improved by adjusting material input values?

To arrive at a reasonable conclusion, this thesis is based on the hypothesis that: gearwheel strength calculation accuracy is probably different with different materials. The calculation is probably too conservative and manufactured gears are overengineered. There is also a considerable doubt that gearwheel strength calculation does not take into account all necessary material properties.

## 2 GEAR CALCULATION METHODS AND THEORY

Theory behind gear calculation and importance of material selection are presented in this section of the thesis. Also calculation method that used software use is introduced.

### 2.1 Material selection

The most used case carburizing steel grades in gearwheels varies slightly between market areas. Wholesale dealers keep just a limited amount of different steel grades in stock and it is financially reasonable to use these grades if possible. It is possible to purchase steel directly from the manufacturer but it usually means that the whole melting patch is bought. Small or medium size companies might have difficulties making this size of investment and storage may be challenging. One steel grade is not enough if the gearwheel size varies widely. One of the main aspects of choosing the right steel to gearwheel is hardenability. Small gearwheels may become thru hardened if unsuitable material is used. In another extremity, large gearwheels may not achieve the required hardening. Typically at least two different materials are used. A different aspect to material choice is the requirement of classifications of material. Every classification costs money and it is a difficult task to choose what classifications should be done when purchasing steel. Knowledge of materials is mandatory when manufacturing gearwheels around the world. It is profitable that the company is capable of recommending suitable steel which is lower price and easier to acquire. This capability needs a deep understanding of how the material affects the strength and usability of the final product.

#### 2.1.1 18CrNiMo7-6

The most common case hardening steel for gearwheels is 18CrNiMo7-6 or W.Nr 1.6587. It is well suitable on bigger parts with a gear module 5 and above. 18CrNiMo7-6 could be delivered in forged bars or cast blanks. The delivery condition depends on bar diameter. Options are Annealed, perlited, or QT. The steel hardness in a delivery condition varies between 190-229 HB depending on diameter. The chemical composition is presented in Table 1.

Table 1. 18CrNiMo7-6 composition

	C	Si	Mn	P	S	Cr	Mo	Ni	Cu
min	0.15	0.15	0.50	0	0	1.50	0.25	1.4	0
max	0.21	0.4	0.90	0.025	0.035	1.80	0.35	1.7	0.4

Hardenability of 18CrNiMo7-6 is presented in the jominy curve in Figure 2. Blue dashed line represents a random sample of the real material certificate from a steel supplier. Grey solid lines represent lower and upper limits of hardness at different depths in the material.

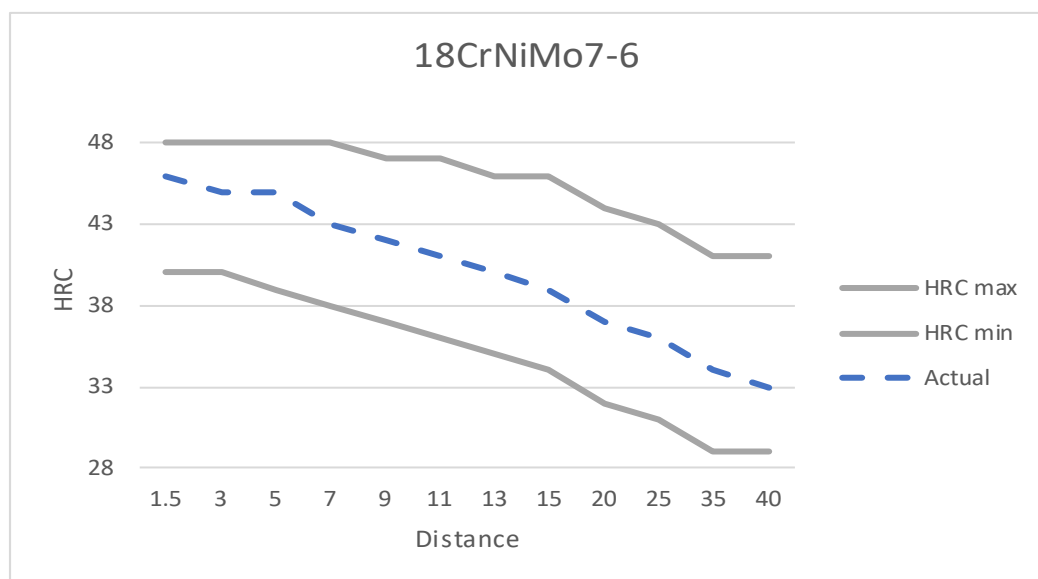


Figure 2. 18CrNiMo7-6 jominy curve with limits

### 2.1.2 20MnCr5

The 20MnCr 5 material is coming more common in gearwheels with a smaller module. Typical use of 20MnCr5 is in gearwheels with tooth size module 5 and smaller. The chemical composition of the material is presented in Table 2.

Table 2. 20MnCr5 composition

	C	Si	Mn	P	S	Cr	Mo	Ni	Cu
min	0.17	0,15	1.10	0	0	1.00	0	0	0
max	0.22	0.40	1.40	0.025	0.035	1.30	0	0	0.40

Hardenability of 20MnCr5 is presented in the jominy curve in Figure 3. The red dashed line represents a random sample of a real material certificate from a steel supplier. Grey solid lines represent lower and upper limits of hardness at different depths in the material.

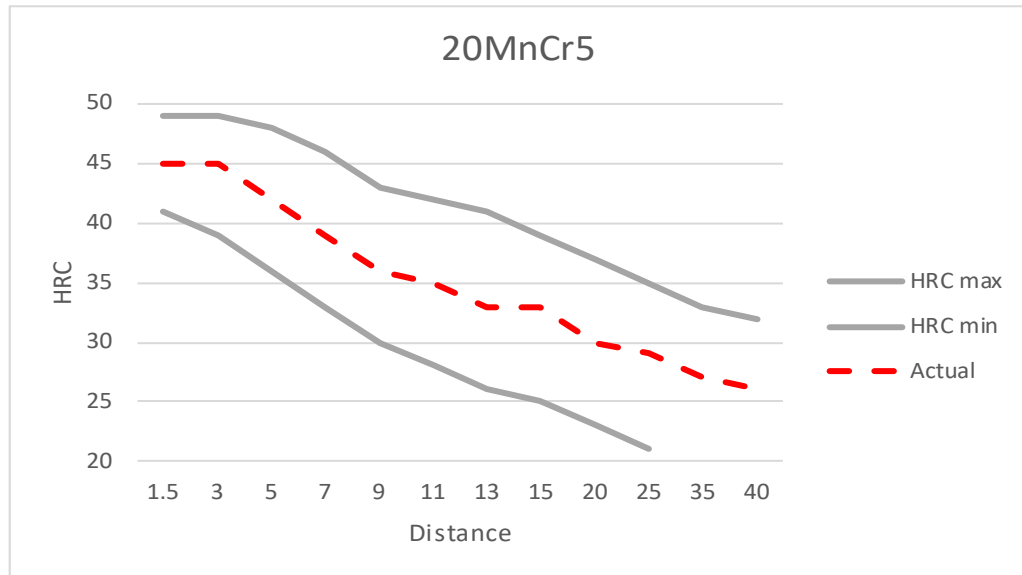


**Figure 3.** 20MnCr5 Jominy curve with limits

### 2.1.3 20NiCrMo2-2

Material 20NiCrMo2-2 is normally used in small tooth gearwheels. Typical use is from module 2 and smaller. Its poor hardenability makes base material be reasonably soft after heat treatment. For this reason common diameters of material bars are smaller than other materials presented in thesis. This material is quite difficult to obtain in size needed in gearwheels used in this thesis. The chemical composition is presented in Table 3.

*Table 3. 20NiCrMo2-2 Chemical composition*

	C	Si	Mn	P	S	Cr	Mo	Ni	Cu
min	0.17	0.15	0.65	0	0	0.35	0.15	0.4	0
max	0.23	0.40	0.95	0.025	0.035	0.70	0.25	0.7	0.40

Hardenability of 20NiCrMo2-2 is presented in jominy curve in Figure 4. Yellow dashed line represents random sample of real material certificate from steel supplier. Grey solid lines represent lower and upper limits of hardness in different depths in material.

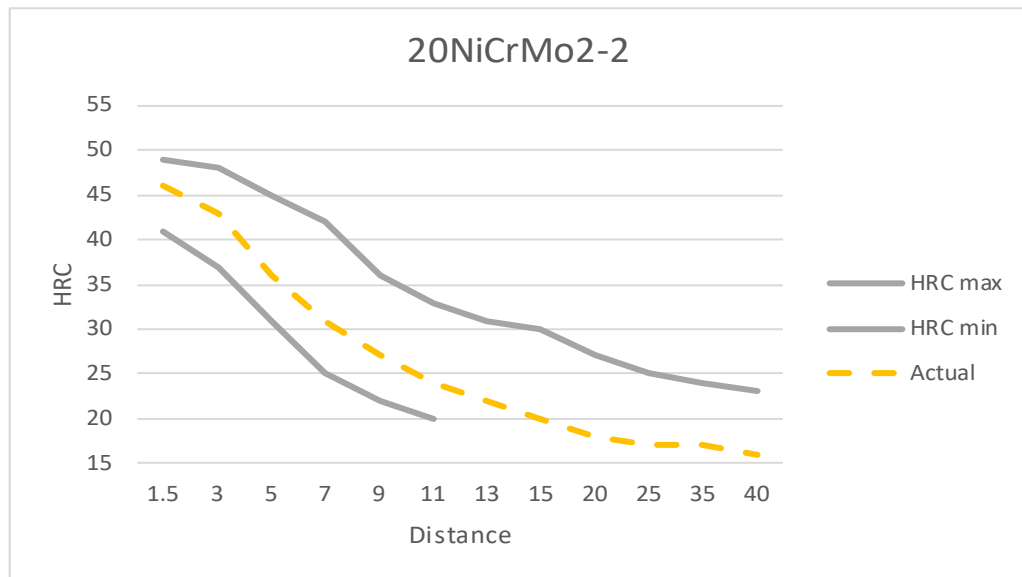


**Figure 4.** 20NiCrMo2-2 Jominy curve with limits

## 2.2 Basic gearwheel calculations

Used gearwheels in thesis are evolvent shaped gearwheels. Used reference profile is defined in standard SFS-ISO 53 (2016, p. 6). Actual root shape of finished gearwheels in thesis is protuberance shape. This allows gear grinding without forming grinding notch. This shape is determined in the tooth cutting tool. Final shape of the tooth is taken into consideration on gearwheel strength calculation.

Gearwheel size is defined as module ( $M$ ) and is expressed as millimeters. SFS-ISO determines recommended modules to use. Tooth size has large impact to gearwheel strength but also physical size. Gearwheel calculations should start with iteration between gear ratio, physical size and power transmission capability. This phase of calculations is called rough sizing in KISSsoft calculation program.

Simplified representation of gearwheel tooth size and shape is shown in Figure 5. Left flank in Figure 5 is protuberance shape and right flank is without protuberance.

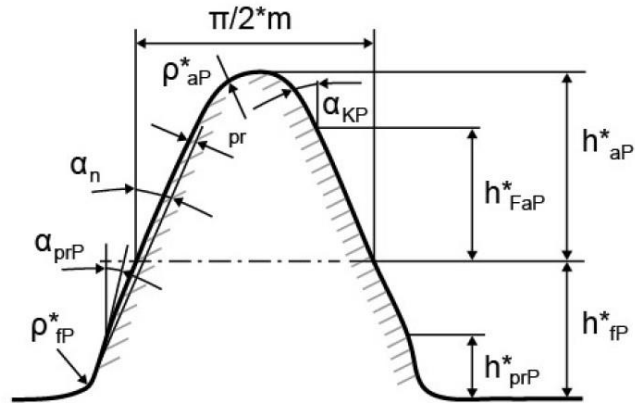


**Figure 5.** Reference profile (KISSsoft 2021, p. 282)

Symbols in the Figure 2 are:

$\rho_{fP}$  root radius

$\alpha_{prP}$  is protuberance angle

$\alpha_n$  is pressure angle

$pr$  is remaining protuberance after grinding

$h_{aP}$  is addendum

$h_{fP}$  is dedendum

$h_{FaP}$  is tip form height

$h_{prP}$  is protuberance height

$\alpha_{KP}$  is profile angle of the chamfer involute

### 2.3 Gearwheel strength calculation

Strength calculations in this thesis are based on standard ISO 6336. This standard determines the principles of strength calculation for spur and helical gears. There are some limitations where equations are reliable. The normal pressure angle must be between  $15^\circ$  and  $25^\circ$ , the reference helix angle must be  $30^\circ$  or less, and the transverse contact ratio should be between 1,0 and 2,5. Also if the gear teeth are pointed, the backlash is zero or there will be interference between tooltips and root fillets, formulae from standard ISO 6336 are not applicable. Gear strength calculations are divided to eleven parts in ISO 6336-1 (2020, p. 6), namely.

- ISO 6336-1 Basic principles

- ISO 6336-2 Calculation of surface durability
- ISO 6336-3 Calculation of tooth bending strength
- ISO 6336-4 Calculation of tooth flank fracture load capacity
- ISO 6336-5 Strength and quality of materials
- ISO 6336-6 Calculation of service life under variable load
- ISO 6336-20 Calculation of scuffing load capacity (Flash temperature method)
- ISO 6336-21 Calculation of scuffing load capacity (Integral temperature method)
- ISO 6336-22 Calculation of micropitting load capacity
- ISO 6336-30 Calculation examples for the application of ISO 6336 parts 1,2,3,5
- ISO 6336-31 Calculation examples of micropitting load capacity

Parts 4, 20, 21, and 22 are technical specifications and not actual international standards. Parts 30 and 31 are calculation examples of previous standards and do not provide added information. The ISO 6336 calculation has three degrees of calculation accuracy. A, B and C. The A is the most precise and the most expensive method of calculation. To benefit from the most accurate A-type calculation method needs an elevated level of understanding of operating conditions, suitable measuring equipment, and extensive research of the relevant relationships. Calculations only are not enough for this method, many factors are tested and determined with real-life measurements of the project in hand. Also cost of all this should be less than the value of gained accuracy. B-method is suitable for most cases. There are some assumptions, and some factors are derived with sufficient accuracy. Method C is based on approximations to allow simplified calculations. This method is suitable in early prototyping or design for offer situations. Also, some low-risk and low force applications are good enough with this method. The used method is presented with additional subscript, e.g.,  $K_{V-A}$ ,  $K_{V-B}$  or  $K_{V-C}$

Other important standards involved are

- ISO 52:1998 which determines basic tooth profile,
- ISO 1122-1:1998 which gives definitions of gear terms
- ISO 1328-1:2013 determines flank tolerance classification

### 2.3.1 Application factor $K_A$

Application factor considers external dynamic actions from different variables. Nominal loads on gears are increased by characteristics of the component masses and stiffness of the entire machine. This includes also shafts and couplings. Method A needs comprehensive analysis of the entire mechanical system and is rarely possible to implement in an early phase of the design process (Vullo 2020a, p. 5). Method B is much more simple and more suitable for the definition of the Application factor  $K_A$ . See Table 4. (SFS-ISO 6336-1 2020, p. 28)

*Table 4. Application factor  $K_A$  for Method B*

Working characteristic of driving machine	Working characteristic of driven machine			
	Uniform	Light shocks	Moderate shocks	Heavy shocks
Uniform	1	1.25	1.5	1.75
Light shocks	1.1	1.35	1.6	1.85
Moderate shocks	1.25	1.5	1.75	2
Heavy shocks	1.5	1.75	2	$\geq 2.25$

### 2.3.2 Internal dynamic factor $K_V$

The internal dynamic factor considers distinctive design parameters like rotating speed, mass and stiffness of rotating parts, lubrication, critical speeds, and vibrations on gears themselves. Also, manufacturing properties are taken into consideration here. Accuracy grade determines maximum deviations as well as determined tolerances in parts and assembly. SFS-ISO 6336-1 (2020, p. 33) Calculation method A needs again comprehensive analysis of the entire system and is possible to use after the machine can be tested. Method B is suitable in many calculations with average accuracy demands. Only when specific sliding is less than 3 m/s method C is preferred (SFS-ISO 6636-1 2020, p. 34; KISSsoft 2021, p. 369.) Specific sliding can be calculated as

$$Ss = \left( \frac{vZ1}{100} \right) \cdot \sqrt{\frac{u^2}{(1+u^2)}} \quad (1)$$

Where

$v$  is circumferential velocity

$Z1$  is the number of teeth of the pinion

$u$  is the gear ratio



$S_s$  is the specific sliding

$K_V$  must be determined in all different running speed ranges. Speed ranges are called subcritical range, main resonance range, intermediate range, and supercritical range in standard ISO-SFS 6336. The main resonance speed can be determined as

$$n_{E1} = \frac{30000}{\pi Z_1} \sqrt{\frac{C_{\gamma a}}{m_{red}}} \quad (2)$$

Where

$C_{\gamma a}$  is mean value of mesh stiffness per unit face width

$m_{red}$  is the relative mass of a gear pair. It can be calculated as,

$$m_{red} = \frac{m_1 m_2}{m_1 + m_2} \quad (3)$$

Where

$$m_{1,2} = \frac{J_{1,2}}{r_{b1,2}^2} \quad (4)$$

$m_1$  is relative individual pinion gear mass per unit face width referenced to the line of action

$m_2$  is relative individual main gear mass per unit face width referenced to the line of action

$J_{1,2}$  is the moment of inertia per unit face width

$r_{b1,2}$  is the base radius

The resonance ratio is used to determine the resonance range. Resonance ratio ( $N$ ) is the ratio of pinion speed to resonance speed and can be calculated as

$$N = \frac{n_1}{n_{E1}} \quad (5)$$

Where

$n_l$  is speed of the pinion in rpm

Main resonance range is defined to be between limits and can be calculated as

$$N_S < N \leq 1.15 \quad (6)$$

Where

$N_S$  is the lower limit

Line loads can be calculated as.

$$w = \frac{(F_t K_A K_\gamma)}{b} \quad (7)$$

Where

$F_t$  is the nominal transverse tangential load at reference cylinder per mesh

$K_\gamma$  is the meshing load factor

Lower limit of main resonance range can be defined as

$$N_S = 0.5 + 0.35 \sqrt{\frac{F_t K_A K_\gamma}{100b}} \quad (8)$$

$$N_S = 0.85 \quad (9)$$

If calculated line loads (specific load per face width) from equation 7 are less than 100 N/mm  $N_S$  is calculated from equation 8. If calculated loads from equation 7 are 100 N/mm or more,  $N_S$  can be calculated from equation 9.

Calculating dynamic factors in different ranges require the calculation of several factors presented in Table 5.

Table 5. Factors to calculate Dynamic Factor (SFS-ISO 6336-1 2020, p. 38)

	$1 < \varepsilon_\gamma \leq 2$	$\varepsilon_\gamma > 2$	
$C_{v1}$	0.32	0.32	
$C_{v2}$	0.34	$\frac{0.57}{\varepsilon_\gamma - 3}$	
$C_{v3}$	0.23	$\frac{0.096}{\varepsilon_\gamma - 1.56}$	
$C_{v4}$	0.90	$\frac{0.57 - 0.05\varepsilon_\gamma}{\varepsilon_\gamma - 1.44}$	
$C_{v5}$	0.47	0.47	
$C_{v6}$	0.47	$\frac{0.12}{\varepsilon_\gamma - 1.74}$	
	$1 < \varepsilon_\gamma \leq 1.5$	$1.5 < \varepsilon_\gamma \leq 2.5$	$\varepsilon_\gamma > 2.5$
$C_{v7}$	0.75	$0.125\sin [\pi(\varepsilon_\gamma - 2)] + 0.875$	1.0

Parameter  $\varepsilon_\gamma$  in table 5 is the total contact ratio and be calculated as

$$\varepsilon_\gamma = \varepsilon_\alpha + \varepsilon_\beta \quad (10)$$

Where

$\varepsilon_\alpha$  is transverse contact ratio

$\varepsilon_\beta$  is overlap ratio

Transverse contact ratio is the ratio between the length of path of rotation and circular pitch and can be calculated as (Vullo 2020b, p. 61).

$$\varepsilon_\alpha = \frac{q}{p} \quad (11)$$

Where

$q$  is length of path of contact

$p$  is circular pitch

Overlap ratio can be determined as

$$\varepsilon_{\beta} = \frac{b \tan \beta}{p} \quad (12)$$

Where

$b$  is face width

$\beta$  is helix angle

Dynamic factor calculations also need three different non-dimensional parameters. and can be determined as

$$B_p = \frac{c' f_{pb \text{ eff}}}{K_A K_V \left(\frac{F_t}{b}\right)} \quad (13)$$

Where

$f_{pb \text{ eff}}$  is the effective base pitch after running-in.

$$B_f = \frac{c' f_{p\alpha \text{ eff}}}{K_A K_V \left(\frac{F_t}{b}\right)} \quad (14)$$

Where

$f_{\alpha \text{ eff}}$  is the effective profile form deviation after running-in.

$$B_k = \left| \frac{c' \cdot \min (C_{a1} + C_{f2}, C_{a2} + C_{f1})}{K_A K_V \left(\frac{F_t}{b}\right)} \right| \quad (15)$$

Where

$C_{\alpha}$  is tip relief

$C_f$  is root relief

Dynamic factor in subcritical range,  $N \leq N_s$ , is calculated as

$$K_v = (NK) + 1 \quad (16)$$

Where

$$K_v = (C_{v1} \cdot B_p) + (C_{v2} \cdot B_f) + (C_{v3} \cdot B_k) \quad (17)$$

Dynamic factor in main resonance range,  $N_s < N \leq 1.15$ , is calculated as

$$K_v = (C_{v1} \cdot B_p) + (C_{v2} \cdot B_f) + (C_{v4} \cdot B_k) + 1 \quad (18)$$

Dynamic factor in supercritical range,  $N \geq 1.5$ , is calculated as

$$K_v = (C_{v5} \cdot B_p) + (C_{v6} \cdot B_f) + C_{v7} \quad (19)$$

Dynamic factor in intermediate range,  $1.15 < N < 1.5$ , is interpolated between values  $N=1.15$  and calculated with equation 18 and  $N=1.5$  and calculated with equation 16. Interpolation can be made as

$$K_v = K_v(N = 1.5) + \frac{K_v(N=1.15) - K_v(N=1.5)}{0.35} \cdot (1.5 - N) \quad (20)$$

### 2.3.3 Face load factors $K_{H\beta}$ and $K_{F\beta}$

Load distribution at the gear tooth contact is never even. Deformation, installation errors, displacements, and manufacturing tolerances cause misalignments and uneven load distribution. Face load factor  $K_{H\beta}$  for contact stress is

$$K_{H\beta} = \frac{\frac{F_{max}}{b}}{\frac{F_m}{b}} \quad (21)$$

Where

$F_{\max}$  is the maximum load

$F_m$  is the average load at the tooth face.

Face load factor  $K_{F\beta}$  for tooth root stress is defined determined from  $K_{H\beta}$  in a similar manner for calculation options B and C from standard SFS-ISO 6336-1, 2020. Calculation of  $K_{F\beta}$  is

$$K_{F\beta} = (K_{H\beta})^{N_F} \quad (22)$$

Where

$N_F$  is determined as

$$N_F = \frac{\left(\frac{b}{h}\right)^2}{1 + \frac{b}{h} + \left(\frac{b}{h}\right)^2} \quad (23)$$

Calculation for  $K_{H\beta}$  is made with method B in standard 6336-1, 2020. Several phases are included and making heavy calculations by computer-aided make sense. Method B includes also iterative actions where hand calculation could take an unreasonably long time. The Flow chart of calculation process is shown in Figure 6.

After dimensions of gears and shafts are acquired, pinion and shaft faces are divided to matching load application stations for shaft bending calculation. Area of gear tooth should be divided into 10 load application increments. Number of increments can be increased if higher resolution is needed, for example when profile modifications is included. Deflections are calculated in all stations independently. Calculation must be done according to actual shape and characteristic of shaft construction. Torsional deflection must also be calculated based on characteristics of actual shaft for torsional twist for hollow cylindrical shaft gives approximation that is reasonable accurate for gearing purposes. Equation takes account only torques from gear tooth loading. Other affecting torques must calculate separately with suitable measures. Torsional deflection can be calculated as

$$f_{\delta i} = \frac{(10^3) \cdot (\sum_{j=1}^i L_j) \cdot (\sum_{j=1}^{i-1} X_j) \cdot 4 \cdot d^2}{G \cdot \pi \cdot (d^4 - d_{in}^4)} \quad (24)$$

Where

$f_{\delta i}$  is the torsional deflection at a station

$L_j$  is the load at a station

$X_j$  is the distance between adjacent stations

$d$  is the effective twist diameter

$d_m$  is the inside diameter

$i$  is the station number

$G$  is the shear modulus

Gap analysis must be done since gear teeth are not fully in contact across the entire face width. Applying load decrease gaps but not always fully to close the gap. Gap analysis is done by summarizing variables that are causing gaps. Bending and torsional deflection calculations give the first two values to sum. Tooth modification for flank line gives a third value if applied. Lead variation is best to find from the measurement of actual gears. Typically, in this phase of designing this is not possible. Tolerances from ISO 1328-1 (2016) can be used to estimate expected variation. Shaft misalignment  $f_{ma}$  can be calculated in several ways depending on application and accuracy demand. With lead variation, also shaft misalignment is best to determine with actual gears by measuring. However, in the design phase, some estimates must be done. Used tolerances can be acquired from standard SFS-ISO 6336-1 (2020, p. 124) and depend on the selected quality class. One approach is presented as

$$f_{ma} = \sqrt{f_{H\beta 1}^2 + f_{H\beta 2}^2} \quad (25)$$

Where

$H_{\beta 1}$  is wheel helix slope tolerance

$H_{\beta 2}$  is pinion helix slope tolerance

The determined gaps can have a positive or negative value. All determined gap values are summarized to achieve a final value of gap analysis.

Load intensity is a result of mesh gap analysis. Target mesh is divided into equal-length increments. The summary of loads in every increment is called total load in the plane of action, BTP. Load intensity can be calculated as

$$L_{\delta i} = \frac{L_i}{X_i} \quad (26)$$

Where

$L_{\delta i}$  is the load intensity

$L_i$  is the load at a specific point

$X_i$  is the length of face where the point load is applied

BTP can be calculated as

$$F_{bt\ eff} = L_1 + L_2 + L_3 + \dots + L_n \quad (27)$$

Where

$F_{bt\ eff}$  is BTP

$n$  is the number of increments

Load intensity difference between points,  $i$  and  $j$ , is proportional. and can be expressed as

$$\frac{L_i}{X_i} - \frac{L_j}{X_j} = (\delta_i - \delta_j)c_{\gamma\beta} \quad (28)$$

All load values can be calculated by modifying this equation.

The last step is to calculate the load distribution factor and this is done by dividing the highest calculated peak load by the average load. Load distribution factor can be calculated as

$$K_{H\beta} = \frac{L_{i\ peak}}{L_{i\ ave}} \quad (29)$$

Where



$L_{i\ peak}$  is highest peak load from load intensity calculations

$L_{i\ ave}$  is average load from load intensity calculations.

Average load  $L_{i\ ave}$  can be calculated as

$$L_{i\ ave} = \frac{F_{bt\ eff}}{n} \quad (30)$$

Flow chart of load distribution calculation order with analytical method is presented in Figure 6. Example of making this calculation in practice is presented detailed in standard ISO 6336-1, 2020 in Annex E.

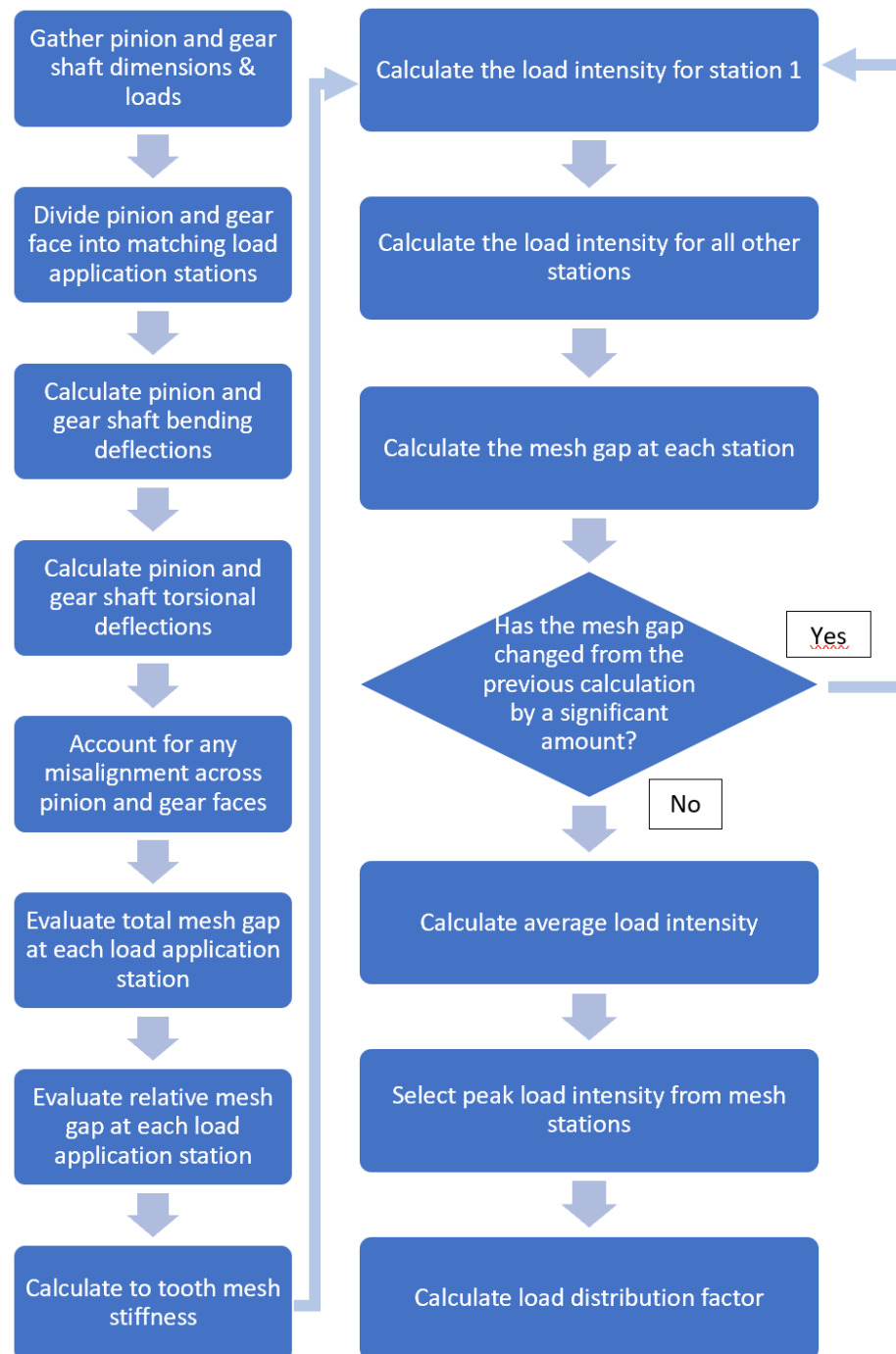


**Figure 6.** Flow chart for analytical method for load distribution. (SFS-ISO 6336-1 2020, p. 133)

Calculation is quite straight forward but needs detailed information as input. Calculations by hand is laborious but preparing equations to suitable calculation software make work faster.

## 2.4 Keyway strength calculation

The standard DIN (Deutsche Industrie Normen) 6885 defines recommended key width. It is not recommended to exceed these widths and if stress is too high, two or more keyways are recommended. The width can be narrower if stress allows it. (DIN 6885-1 2021, p. 4). The length of the key should be calculated after the key width and height are decided from the standard. Two different stress types must be taken into consideration, shear stress and bearing stress. Shear stress can be calculated as

$$\tau = \frac{2T}{dbL} \quad (31)$$

where

$\tau$  is shear stress

$T$  is applied torque

$d$  is shaft diameter

$b$  is the width of the key

$L$  is the length of the key.

In terms of yield strength and safety factor, the key length is

$$L_{\tau} = \frac{2Tn_{\tau}}{dbS_{sy}} \quad (32)$$

Where

$n_{\tau}$  is the safety factor

$S_{sy}$  is yield strength.

Bearing stress can be calculated as

$$\sigma = \frac{2T}{0.5dhL} \quad (33)$$

Where

$h$  is the height of the key.

Adding yield strength and safety factor, results final equation for key length as

$$L_{\sigma} = \frac{2Tn_{\sigma}}{0.5dhS_y} \quad (34)$$

Where

$n_{\sigma}$  safety factor

$S_y$  is the tensile yield stress limit

For key length, the larger result from Equations 33 and 34 should be chosen. The length of the keys described in standards should be used. Other lengths can be used but they must be manufactured for the case.

## 2.5 Gearwheel manufacturing

Used gearwheels are manufactured with standard tools typically used in industry. Next operations were included in the manufacturing process.

- Sawing
- Turning
- Hobbing
- Deburring
- Heat treatment
- Grinding
- Gear grinding
- Inspection

The most critical parts of gearwheel manufacturing are hobbing, heat treatment, and gear grinding. Other phases don't have so critical an effect directly on tooth strength.

### 2.5.1 Hobbing

Gearwheel tooth cutting is possible in several ways. Hobbing has proved to be one of the most efficient ways of manufacturing gears. Hobbing tool is formed by shaped cutting teeth in spiral form. (Figure 7) (Vullo 2020a, p. 133.) Cutting gears with hob is possible with

lathes and machining centers but typically just on a very small scale. Dedicated hobbing machines are fast and efficient to cut teeth both, single gears and a larger patch of gears (Vullo 2020, p. 133).

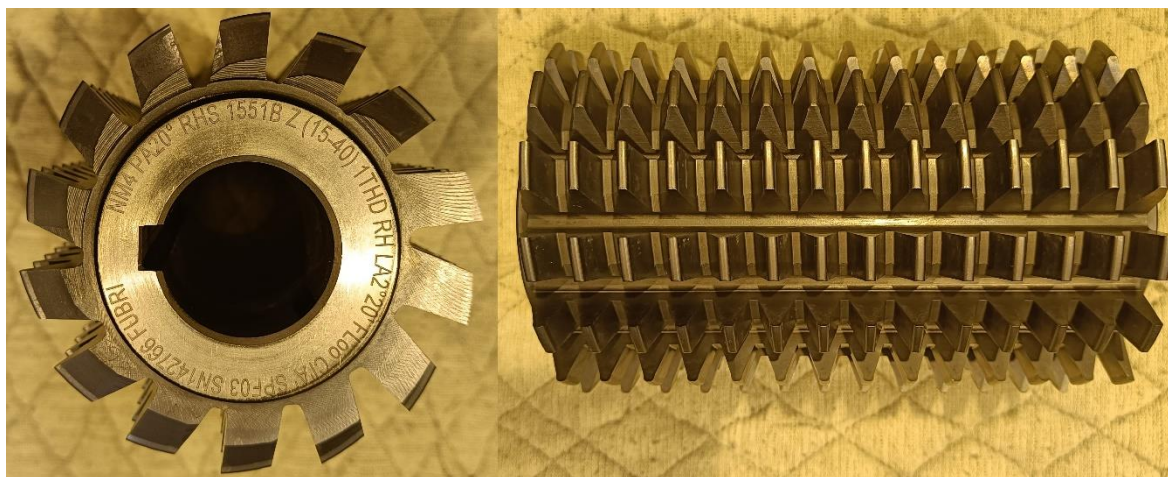


**Figure 7.** Hobbing tool used to manufacture gearwheels designed in thesis

Hobbing tool has a profile form that is not easily modified. The drawback of this kind of tool is its lack of versatility. Every module, pressure angle, and flank profile need its hobbing tool. Fact that most of the most demanding gearwheels are ground after hobbing makes this method more profitable. In these situations shape that hobbing tool typically makes is called protuberance. This means small relief in the tooth root area that allows gear grinding without forming a grinding notch. Protuberance size and shape is not fully defined in standards. Protuberance angle should be 8 degrees or more or the cutting edge of the tool could be too small. (Kapelevich et al. 2019, p. 632.) Different depths of protuberance is used in depending of expected deformations in heat treatment or demanded amount of protuberance after grinding. (SFS-ISO 53 2016, p. 16). In some cases shape with no protuberance can be used but forming grinding notch must be taken into consideration in gear strength calculation.

### 2.5.2 Heat treatment

The heat treatment method of used gears is case carburizing, sometimes called case hardening. Case carburizing can be done in several different furnace types. Two widely used furnace types are box furnace and pit furnace. Both furnace types give the same hardening result but have different features and may cause different stresses and deformations to the

workpiece. Every material has its unique heat treatment program. This program varies to give wanted results and is dependent on used individual furnaces. The same program typically gives slightly different results in different furnaces. (Kivivuori 2016, p. 46.) One of the reasons for this thesis is to find how programs and furnaces meet with theoretical calculations in the target company. All used materials act similar way but results are different due to different compositions.

Case carburizing is a surface hardening method. Used material contains very little carbon and so hardenability is quite poor. Carbon needed in the hardening process is delivered from the atmosphere in the furnace. This is a very well-controlled process. Imported carbon sink in to surface of the steel, and cause hardening when quenched. The depth of the hardened layer is controlled by the amount of carbon in the atmosphere and the time given carbon to diffused in steel. (Kivivuori 2016, p. 45.) This method makes it possible for to surface of the gearwheel tooth to be very hard. At the same time center of the tooth could be much softer and give good toughness (Maláková et al. 2019, p. 1). Problems could occur if hardenability is too good, and the center of the tooth becomes too hard and fragile. This is a typical problem in smaller teeth. Big teeth could have problems if hardenability is not enough. In this case, it is possible that hardening is not happening. Mass of the tooth could reduce cooling speed too low in quenching. These are valid reasons to use different materials even if their reported strength is very similar (Kivivuori 2016, p. 21).

### 2.5.3 Gear grinding

The gearwheel tooth shape is typically finished with gear grinding. Two major methods are profile grinding and generating grinding. Profile grinding uses a cylindrical grinding wheel. Dressing wheels are used to shape the grinding wheel as needed (Davis 2005, p. 117). The dressing process is versatile and most of the limits come from machine moving limits. Grinding is done one tooth at a time. In most cases, both flanks of the tooth are ground simultaneously, but special shapes or very wide tooth gaps can be ground one flank at a time. Generating grinding uses a grinding wheel with spiral forms, like a hobbing tool. (Davis 2005, p. 118.) In generating grinding gearwheel and grinding wheel are spinning simultaneously. This makes the grinding process much faster compared to profile grinding. Because of the larger grinding wheel, dressing takes a longer time. In most cases, it is

possible to grind several workpieces with one dressing. Dressing tools are typically formed to fix shapes to lower the dressing time (Davis 2005, p. 119). Although this makes dressing faster, it prevents to make modifications to the gearwheel tooth profile. Generating grinding is more proficient in larger patches and profile grinding in single workpieces and small patches. Choosing the right grinding method and dressing tool has a significant impact on manufacturing costs and one method is not always better than another. Grinding machines with the ability to use both methods are in the market and are capable of utilizing the best features from both worlds (P90G 2021).

## 2.6 Expected damage mechanisms

Gearwheel could damage several ways during operation. Test arrangement is designed so that there should be only material failures. The static test is exceeded in a controlled way. This gives comparable results to calculations. Dynamic test results are more unpredictable and the damage mechanism is not known beforehand. Pitting and scuffing are most expected but tooth flank or root fracture is also possible. About 40% of gearwheel damages occur in the active flank of the gearwheel (Jelaska 2012, p. 166).

### 2.6.1 Pitting

According to Terrin et al. (2018, p. 2321) pitting is one form of contact fatigue failure. Repetitive contact stress causes craters to the tooth flank surface. Craters are failure points to tooth destruction and cause noise and vibration in an earlier stage. Pitting can be divided to micropitting which is visible to the naked eye only when several micropits form a matt surface. Macropitting is possible to see and crater size is about 0,5 to 1 mm. Several micropits could cause also bigger parts to separate from the flank and thus cause larger problems. 14% of all gear damage is caused by pitting (Jelaska 2012, p. 166).

The gearwheel in Figures 8 and 9 is taken from a used gearbox during routine maintenance. The gearbox was at the end of the designed lifetime and several pitting damages are seen on both flanks. The pitting pattern indicates that contact is not similar on all surfaces of the flank. This gearwheel could benefit from helix angle modification. Helix angle changes a little bit due to shaft bending, bearing deviation, and other variables. It is possible to calculate needed correction if the given data is accurate enough. The exact time of usage of gears in

Figures 10, 11 and 12 is not clear. Used gearbox has irregular using periods and no measurement for operating hours. Gearbox came to maintenance due to larger maintenance operations in the factory. Besides pitting there is clear signs of wearing in the tooth flanks.



**Figure 8.** Pitting in gear flanks

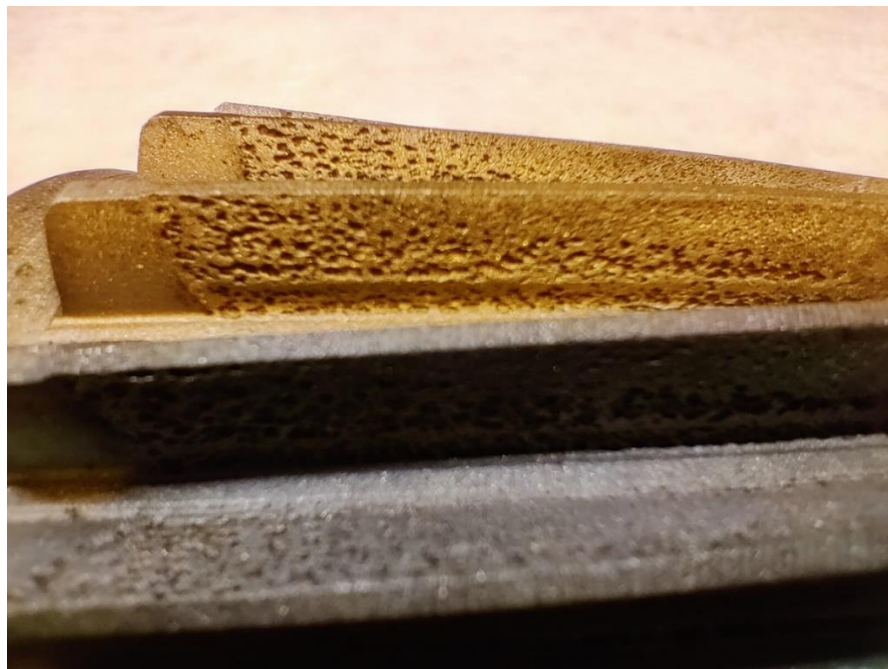


**Figure 9.** Close up from gear flank



The tooth flank area is not used all the way and the counter wheel shape is visible. Typically, the pinion flank width is slightly larger than the counter wheel. This is to prevent any loss of contact area if gears are slightly mislocated in the gearbox. This leaves little playroom for assembly personnel to adjust bearing clearings and other important measures.

### 2.6.2 Scuffing

Scuffing is adhesive wear in its most destructive form. It is happening when lubricating oil film is penetrated fully and micro-welding of tooth flank occur. This weld is torn apart, and a small amount of material is separated from the tooth. This form of failure is seen first at the root and tip of the tooth, where most sliding is happening. Flank sliding causes marks from torn micro-welds to be longer and more visible. The insufficient load capacity of lubricant is the root cause of this failure. Overloading or elevated temperature could cause scuffing in an otherwise correctly designed gearbox (Jelaska 2012, p. 213).

Figures 10 and 11 show an example of scuffing damage. The gearwheel was taken out from a completely broken gearbox. The cause of the damage was significant overload. In this case, operating time was just some days. Overloading was happening most probably due to calculation errors or wrong input values in calculations. Signs of scuffing are visible which indicate lubrication problems or too high tooth flank stress. Since the possibility of lubrication problems was eliminated within the study, overloading is the probable cause.

Since contact stress was remarkably high also severe pitting has occurred. This pitting would cause critical damage very soon.



**Figure 10.** Scuffing and pitting damage in gear flanks



**Figure 11.** Detail from Figure 6 showing pitting damage on gear flank near root and scuffing near tip diameter

Counterwheel for the previous pinion is shown in Figure 12. Some teeth are completely torn away. The definitive reason for this is not certain but clear is that strength of the material is exceeded. Teeth still in place have little or no pitting damage. This indicates that failure occurred quite fast.



**Figure 12.** Gearwheel with damaged teeth

One theory is that pinion in Figures 10 and 11 have lost some material due to pitting and that material ends up between flanks and caused crack. This could escalate quickly and cause damage as shown in Figure 12.

### 3 RESULTS AND DISCUSSION

All results from work in thesis and discussion are in this section of the thesis. Details of the design parameters are also presented in this section.

#### 3.1 Gearwheel design specifications

Gearwheel design was made with the KISSsoft calculation program. The base calculation was made in KISSsoft, however the manufactured gearbox is based on a KISSsys and KISSsoft model of the gearbox in production. This model was altered to match the real situation in this test. The changed part was the side shaft and phase two main shaft. The original design has two gear ratios with automatic gear change. Gear shift and synchronizing related parts were removed from the model. Gearwheel size was chosen to be M4. Module was chosen based on earlier experience, in this size material selection is not trivial and more than one material could be suitable. Also, this size is possible to design to reasonable lifespan for full-time tests with the power we can provide. The test system is equipped with two identical electric motors and is capable of 2000 Nm torque at 2100 RPM. The total transmission ratio of the test bench to the tested gearbox is 1.95. The measured loss of power is roughly 15%. The transmission ratio in the second unchanged gearwheel pair in the test gearbox is 0.5. Preferable transmission ratio to tested gearwheel pair is 1-1.2. The reason for this is to maximize torque from motors without exceeding the maximum speed of motors.

Tip diameters of gearwheels are limited by measures of the gearbox. The root diameter of gearwheels is limited by the required diameter of used shafts. Tip diameter limits are roughly  $\text{Ø}250$  to the first gearwheel and  $\text{Ø}260$  to the second gearwheel. Since gearwheels are interacting exact limits are depending on the opposite gear. The diameter of the center hole of the first gearwheel was decided to be  $\text{Ø}125$  mm. This is for making for make possible to remove the gearwheel from the shaft without removing the bearing. Construction of shaft for first tested gearwheel is shown in Figure 13.

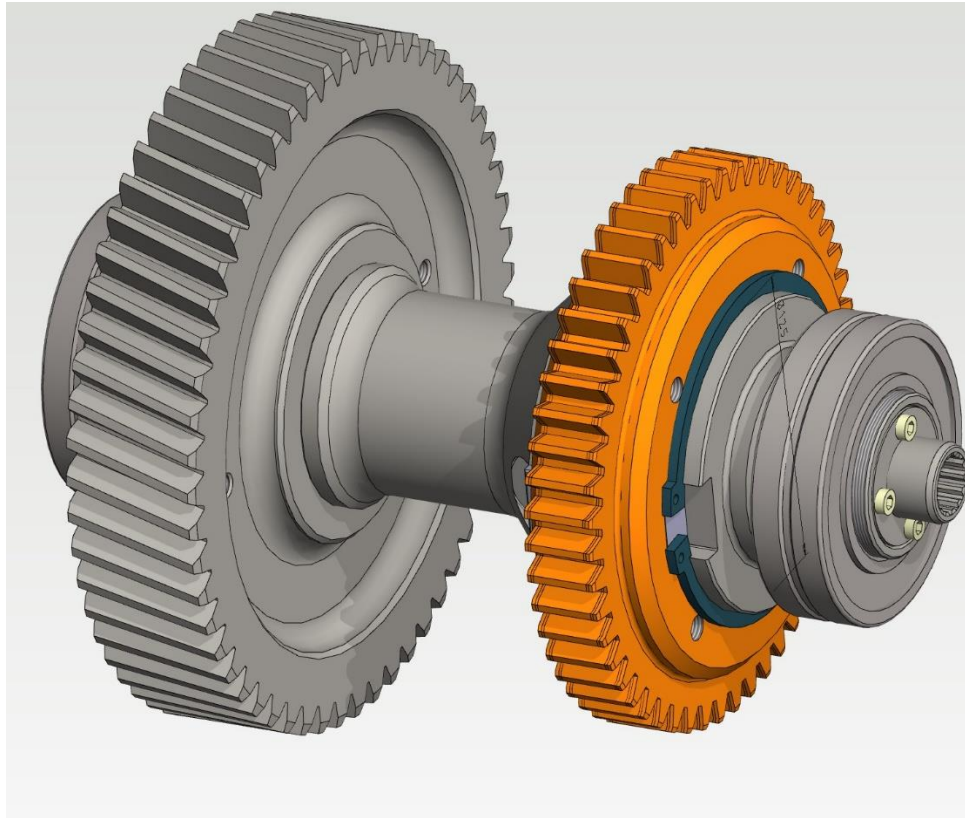


**Figure 13.** Shaft assembly for first tested gearwheel

The diameter of the center hole of the second gearwheel was determined by the size of the necessary key. The needed diameter was  $\text{Ø}85$  mm. Construction of shaft for second tested gearwheel is shown in Figure 14.



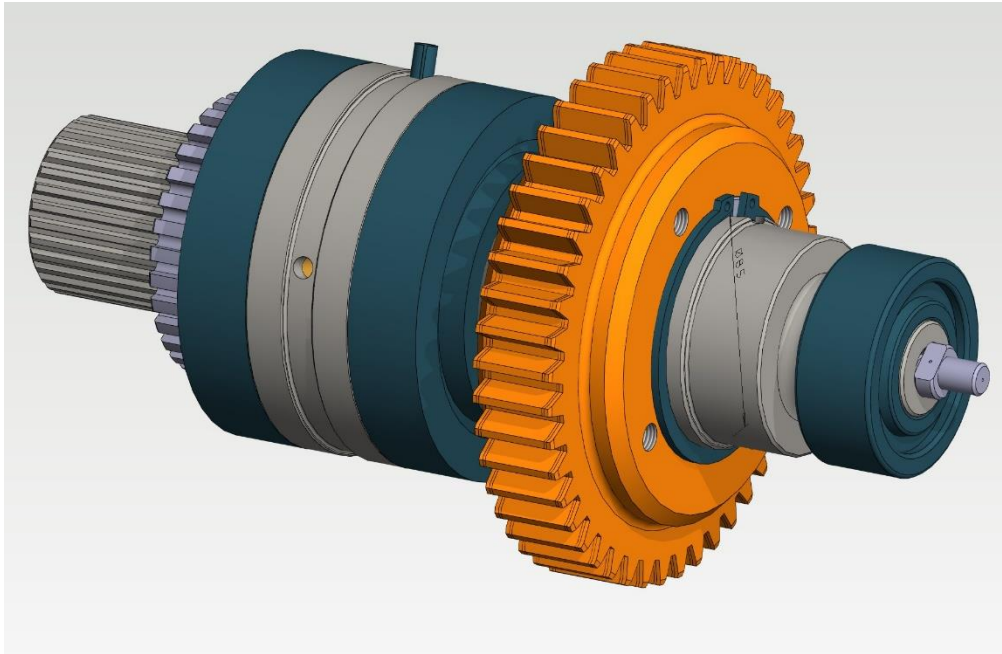


**Figure 14.** Shaft assembly for second tested gearwheel

Input values in KISSsys calculations for speed and torque are presented in Table 7. Blue value presents calculated service life to tested gearwheel pair.

*Table 6. Input values to KISSsys for speed and torque*

	Speed [rpm]	Torque [Nm]	Power [kW]
Input	760	2200	175.09
Output	1294.8	-1266.3	171.7
	minSF[-]	minSF[-]	ServiceLife
z1z3_Calc	1.97	1.13	1.29E+25
z2z4_Calc	1.01	1.17	8.38

The desired lifetime of the gearwheel pair was achieved by iterative process with using KISSsoft fine sizing feature and adjusting face width value manually in calculation. Face width in gearwheel two was determined to be 3mm wider than gearwheel 1. This is to prevent undesired face load due to machining and installation errors in gearwheel positions in the gearbox.

KISSsys model of the gearbox was given finished to make necessary modifications according to test designed in thesis. Used model was missing few elements from calculation,

for example case stiffness, but model is same in the calculations between materials. Since the model remains same these variables are not relevant. Lubrication method is oil bath lubrication and used oil is Shell Omala S2 GX 100. All shafts are manufactured from 42CrMo4 steel. Casing material is AlSi7Mg aluminum alloy. Temperatures in calculation are based of actual measurements of original gearbox. Housing temperature is 67°C and shaft temperature 72° C. Oil temperature in calculation is 70° C.

### 3.2 Gearwheel calculation process

Goal was to calculate gearwheel pair to limited lifetime to make full lifetime testing possible in reasonable testing time. Limited lifetime of gearwheels was achieved by adjusting width of the tooth. The gear ratio was changed to desired and thus shaft diameters were changed. Also, fitting diameters were increased since gear was fixed to shaft with keys instead of a shrink fit. Diameter tolerances between shaft and gears were determined to the smallest amount of shrink fit as possible. This centers gearwheels to shafts but makes changing gears as easy as possible. The shaft diameter and gearwheel hole came quite large relative to the size of the teeth. Used torque was still high and slight oversizing prevents any deformations in the key or the keyway. This again makes assembly and disassembly easier.

Typically, the calculation process starts with the rough sizing of gearwheels. In this case, the module was decided to be four and helix angle zero. This makes it reasonable to start with fine sizing. In fine sizing process in KISSsoft makes it possible to input limits to possible results. The main limits are the gear ratio, tolerance, center distance from the gearbox, maximum tip diameter to fit in the gearbox, minimum root diameter to keep enough distance to the shaft. Module and pressure angle were predetermined due to manufacturing demands. Helix angle was zero. The number of results depends on input limits. Choosing the best solution is depending on calculation goals. Results may include possibilities that are difficult or impossible to manufacture with existing tools. Results can be also arranged to find for example predictable most quiet version. The final decision in the thesis was made by narrowing possibilities to include just small positive profile shift solutions due to easier manufacturing. A secondary criterion was low power transfer capability, and the final decision was made by choosing most silent option.



### 3.3 Results of gear strength calculation

As expected, varied materials give different lifetime results when other factors remain the same. Final calculations were made to achieve similar lifetime to make physical testing possible in reasonable time. This was done by adjusting width of the tooth so that desired calculated lifetime was achieved. In comparative results used gearwheel widths are similar as final calculations with material 18CrNiMo7-6. First gearwheel tooth width is 16 mm and second gearwheel tooth width is 19 mm. Hardening depth is usually company specific parameter. Hardening depth used in this thesis was 0.6+0.6 mm and surface hardness  $60\pm 2$  HRC. Speed and torque are inputted to gearwheel 2 are 760 RPM and 2200 Nm, respectively. These values were determined from testing capability of test bench. Input locations of power values were determined how KISSsys model was built. Quality grade of gearwheels was determined to be 5 by standard ISO 1328:1995. High accuracy prevents variation from manufacturing, but this quality grade is still relatively easy to manufacture with machines in hand. Only modification to teeth are chamfers on tooth edges. Tip chamfer has amount of 0.3mm and angle  $45^\circ$ . Face chamfers are 1mm and  $75^\circ$ .

Calculated safety factors to root and flank for gearwheel pair made with 18CrNiMo6-7 steel are shown in Figure 15. Expected damage is happening in gearwheel 1 root after 8.38 hour. Gearwheel 2 root and flanks of both gearwheels are very close to each others.

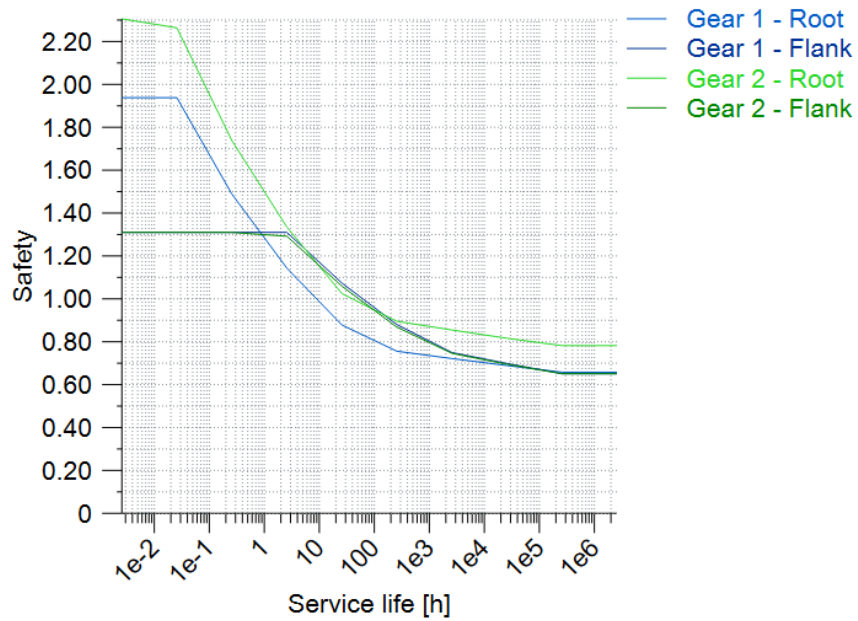


**Figure 15.** Calculated safety for gearwheels in 18CrNiMo7-6 steel

Similar safety factors calculated with material 20MnCr5 gives results shown in Figure 16. Expected lifetime is 2.32 hour in gearwheel 1 root. Flank safety in both gearwheels is slightly larger than gearwheel 2 root safety.

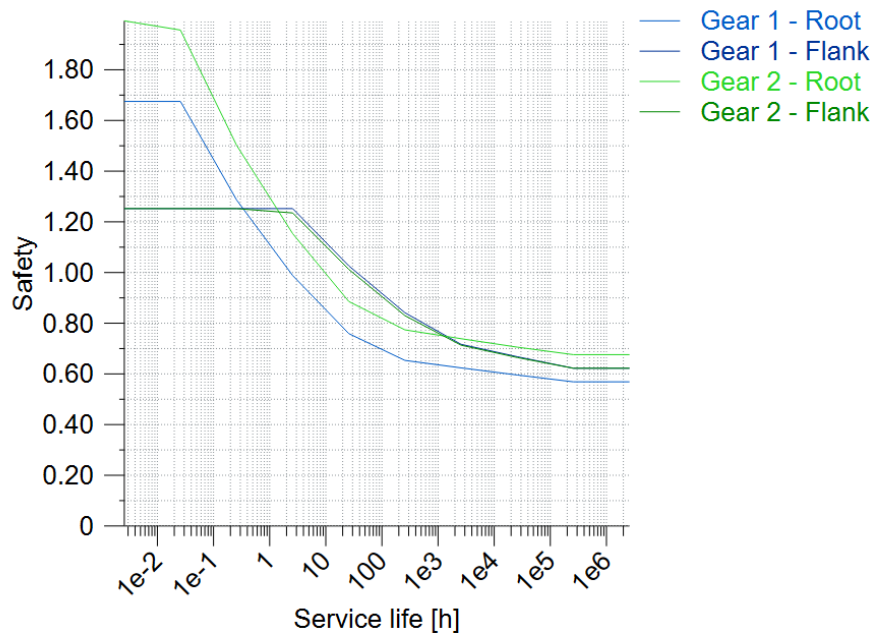


**Figure 16.** Calculated safety for gearwheels in 20MnCr5 steel

Calculated safety with material 20NiCrMo2-2 is shown in Figure 17. Lifetime expectation of the root of gearwheel, one is just 1.16 hour and flank safety is larger than previous materials.

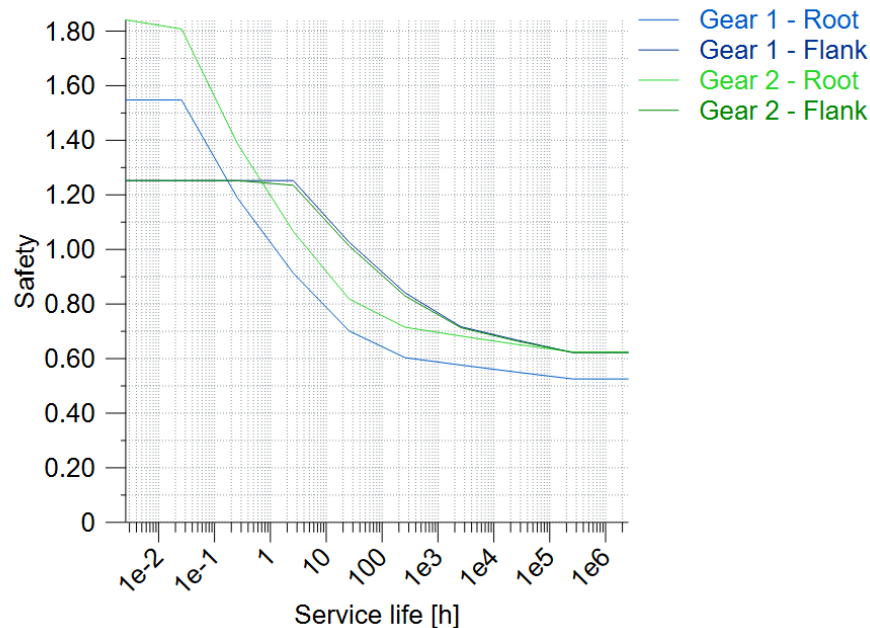


**Figure 17.** Calculated safety for gearwheels in 20NiCrMo2-2

It is noticeable that material strength affect expected lifetime, but also has some effect to failure mechanism. 18CrNiMo7-6 first gearwheel root has clearly lowest lifetime comparing to flank or second gearwheel flank and root. Gearwheel 2 root strength comes relatively stronger comparing to flank when changing steel with lower strength.

Tooth root strength is most critical part of the gearwheels designed for this thesis. Calculated tooth root stresses are presented for more critical gearwheel, gear 1 or A. Analysis at critical point at 30° tangent shows stress spike at the end of the tooth flank. (Figure 18) Adding even one micron of gear flank crowning modification removes peak value. Effect to expected lifetime is marginal, approximately 3%. It is critical to understand calculation results. This kind of stress peaks might look critical but might be avoided quite easily and could be almost left unnoticed. On the other hand manufacturing deviations could easily cause this kind of anomalies when recalculating.

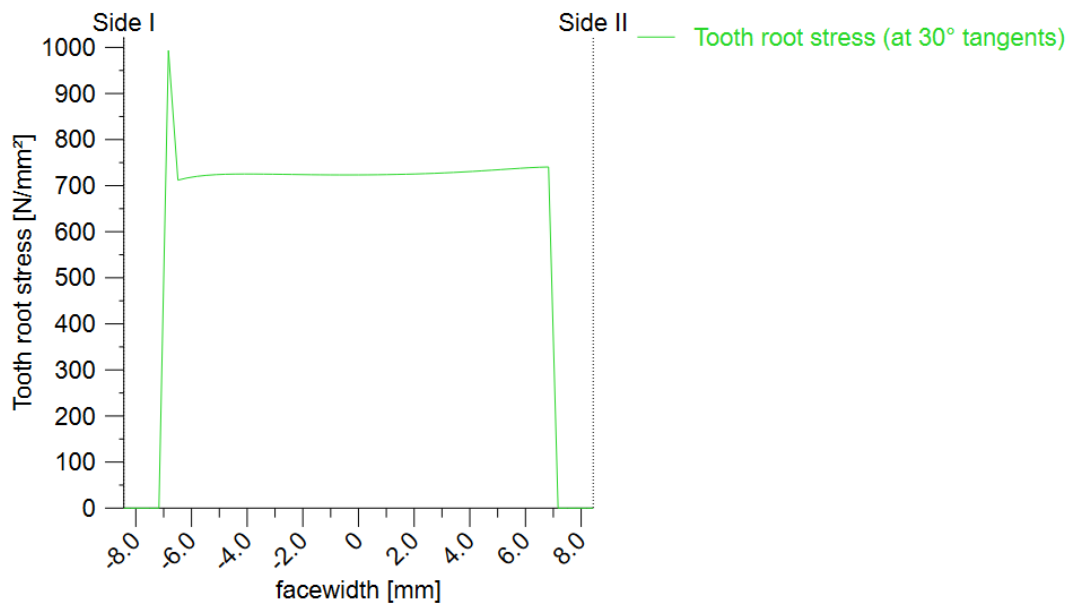


**Figure 18.** Stress on root across face width

Material changes between 18CrNiMo7-6, 20MnCr5 and 20NiCrMo2-2 does not affect root stresses as shown in Figure 19 for 18CrNiMo7-6. Since the stress remains the same, material properties must explain differences in calculated lifetime.

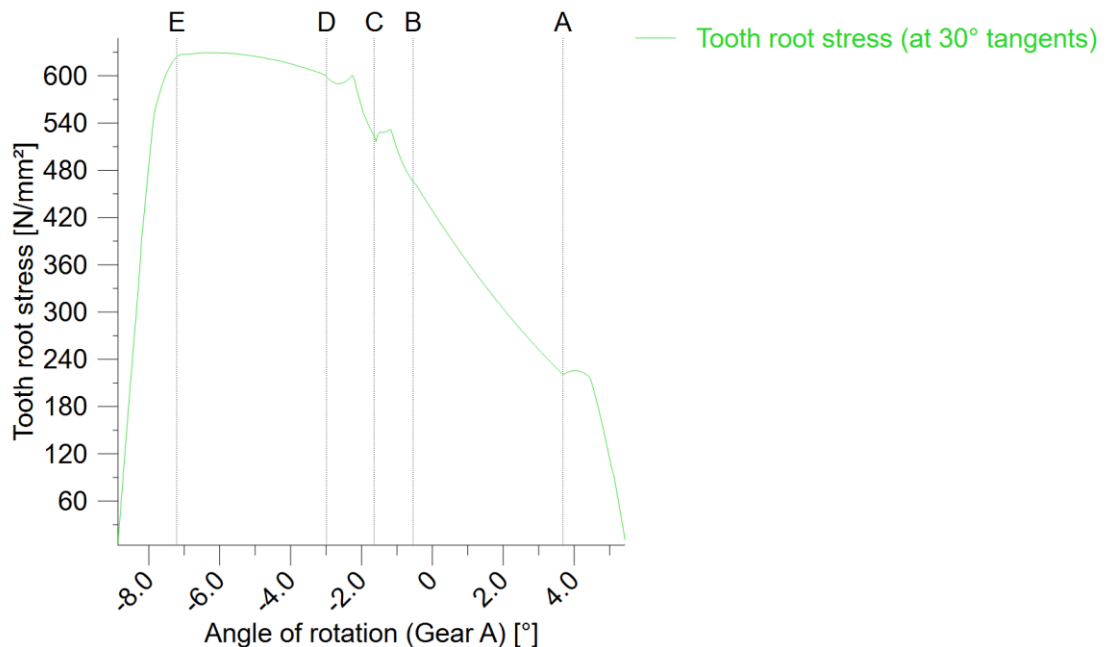


**Figure 19.** Tooth root stress 18CrNiMo7-6

Location of tooth root stresses remains same between materials 18CrNiMo7-6, 20MnCr5 and 20NiCrMo2-2. It clearly noticed from Figure 20 where highest values of the tooth root stress are located.

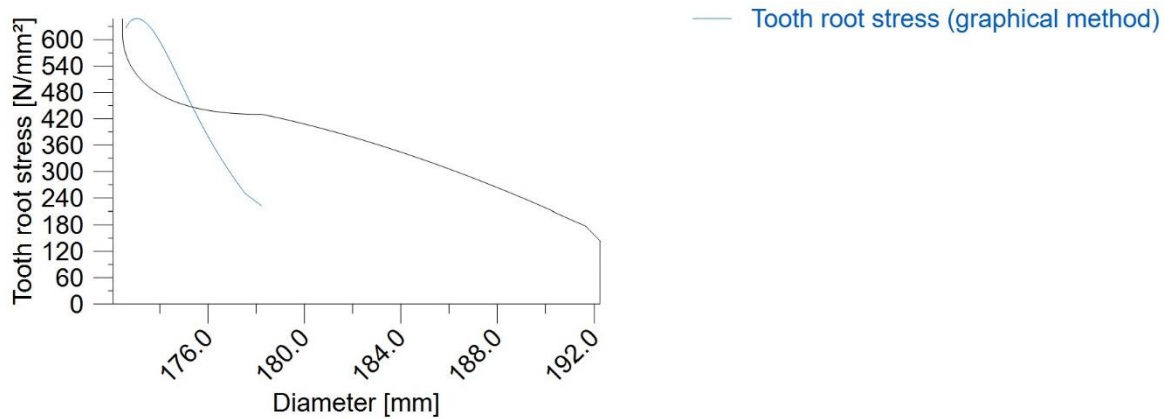


**Figure 20.** Tooth root stress location

Load distribution is not optimal. Figure 21. Most of the load is focused to both ends of the tooth. Changing material does not have an effect on load distribution.

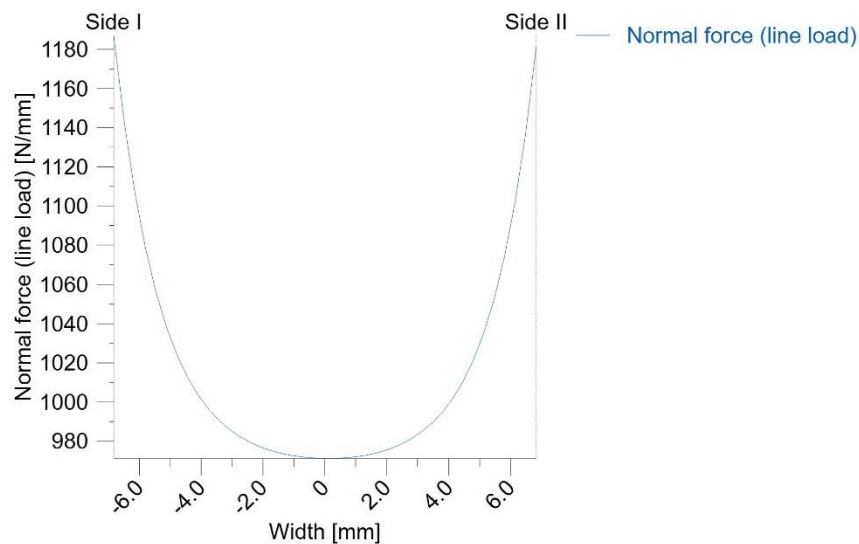


**Figure 21.** Load distribution at the operating pitch circle 18CrNiMo7-6

Adding 8 $\mu$ m flank line crowning modification gives result shown in Figure 22. Load distribution is much more even and highest load is smaller. Effect to calculated lifetime is 9,3%. Tolerance of tooth face form with accuracy grade 5 in calculated gear is 5,5  $\mu$ m. These

modifications in microgeometry have significant effect on stress and strength. Manufacturing tolerances might be much larger because of lower demands in accuracy grade.

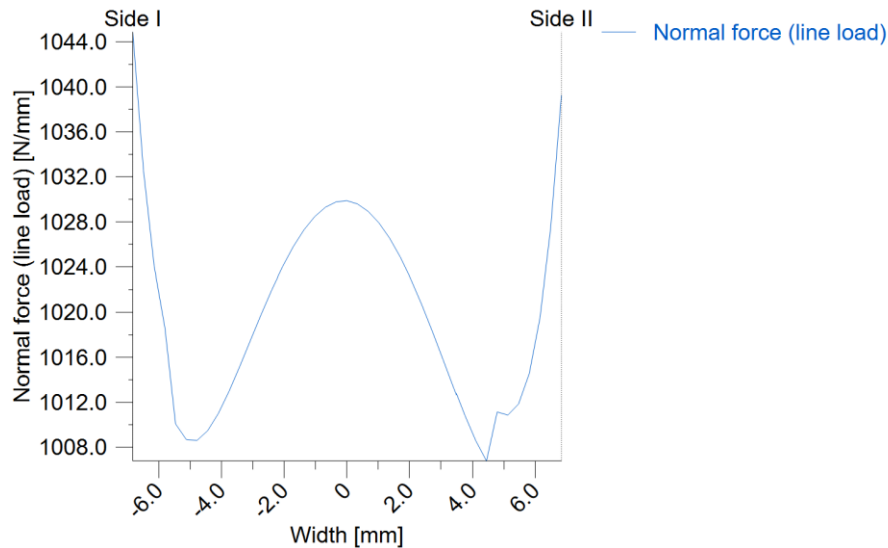


**Figure 22.** Load distribution in the operating pitch circle 18CrNiMo7-7 with flank crowning

### 3.4 Gearwheel manufacturing

Hobbing was made with special tool specified by Katsa. Evolvent shape is directly from standard, but shape of the root and size of the protuberance are specially chosen to fulfill most of the needs in Katsa manufacturing. Hobbing process produces basic shape of tooth. Geometry of tooth and root area is same in every gear and is not point of interest in this research. Used root shape is called protuberance. Protuberance is undercut in root area of the tooth. Purpose of this is to allow grinding without leaving a notch. Typical used protuberance angle is  $10^\circ$ . This is possible to determine in design phase. Protuberance shapes used in Katsa are  $10^\circ$  and every other angle needs new hobbing tool or different manufacturing method.

Used hobbing tool is named as RHS15-40. Tool makes protuberance shape with grinding allowance in gear flank. (Figure 23)

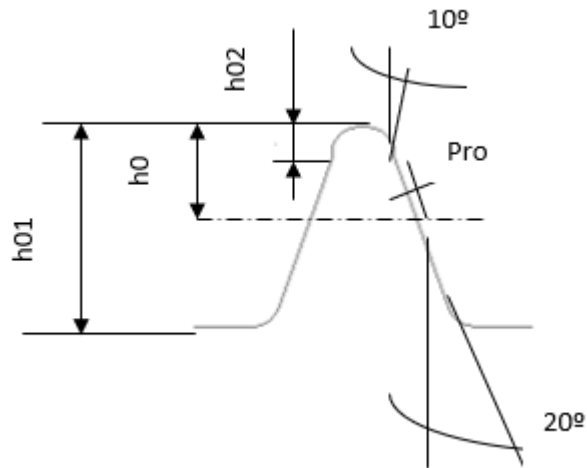


**Figure 23.** Protuberance shaped hobbing tool

Protuberance depth depends on module,  $m$ . This is maximum grinding allowance without grinding notch. Actual grinding allowance must typically be smaller due to machining errors and deformations in heat treatment. Protuberance can be calculated as

$$Pro = 0,15 + 0,02 \times m \quad (35)$$

Protuberance height is determined as

$$h02 = 0,33 \times m + 0,85 \quad (36)$$

Addendum of the hobbing tool determines dedendum of the gear tooth and final depth of the gear tooth. Addendum of the hobbing is tool is determined as

$$h0 = 1,25 \times m + 0,25 \times \sqrt[3]{m} + \frac{Pro}{\sin \alpha} \quad (37)$$

Tooth length is critical if out diameter of gear is larger than normally. This may be case If profile shift is large or for some reason tolerance position of out diameter is abnormal. Tooth length affect strength of the tool, similar way than in the gearwheel. Hobbing tool tooth length is compromised of usability and durability. Full length of hobbing tool tooth is determined as

$$h_{01} = h_0 + 1,3xm \quad (38)$$

Final shape of the tooth is produced in gear grinding. Katsa use two different methods of gear grinding, profile grinding and generating grinding. Both have benefits and drawbacks.

Profile grinding allows unique evolvent profile on each flank of the tooth. Small corrections and bigger reliefs or other shapes are easy to manufacture and compensate. Method is very versatile and does not have too many limitations. However, dressing must be performed quite often since grinding is always happening in same part of the grinding wheel. Also grinding is done one tooth at a time.

Generating grinding use grinding wheel with helical grooves, similar than hobs. Grinding wheel and workpiece rotate in synchronization. Dressing took longer than in profile grinding but in most cases it is possible to grind several workpieces with one dressing. Grinding wheel oscillates all the time so grinding is happening with the fresh wheel in all given time.

In comparison, best case scenario to profile grinding is just few big, long teeth. Generating grinding is best when there is lots of smaller, shorter teeth. In real life patch size, gearwheel size and of course workload of machines determine best method. There are just few limitations when other methods are not available. They are regarding machines, usually not method itself. For example, size limitation of Reishauer RZ1000 is Module 10 and outside diameter 1000 mm. Gleason Pfauter profile grinding machines are not capable to grind smaller diameter than basic diameter. This is mandatory in some exceptional cases where number of teeth is very small  $Z > 10$  and module is big  $M > 9$ .

The critical aspect in gear grinding is if grinding notch is forming. Grinding notch is forming if protuberance form is not used or if grinding allowance is not large enough and protuberance is grinded of. Location of grinding notch is the most important aspect to notice. Figure 24 shows where largest tooth root stresses are located. It is not allowed to form grinding notch in this area. In a typical situation in component manufacturing, this stress distribution chart is not available. Standard SFS-ISO 6336-3 (2020) determines that most vulnerable part of tooth root is determined by line at  $30^\circ$  from tooth centerline tangent to



root radius. In most cases it is enough that grinding notch is not in this area. However in more critical applications notch effect must be calculated according to specific place of grinding notch.

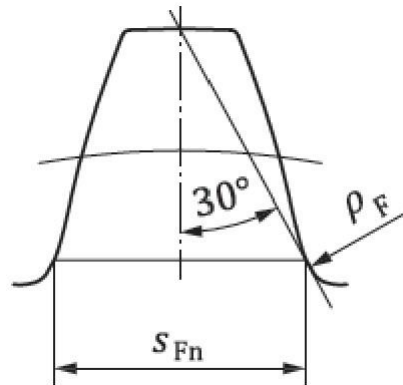


**Figure 24.** Determine of 30° tangent location of tooth root (SFS-ISO 6336-3 2020)

Drawings of gearwheels are in Appendix 1, 2, 3 and 4

### 3.5 Dynamic test bench design specifications

The existing test bench was not suitable to perform the designed test and needed additions. Existing test bench include two Visedo PDR-Me-2100-T1900-DUAL electric motors and three gearboxes. Maximum torque of motors is 2000 Nm at 2100 RPM in this installation. Two of the gearboxes are equipped with two stages and are electrically guided. This makes it possible to change the ratio during tests. System is possible to use manually with computer or via CAN-bus with predefined commands. In the beginning the test system was capable of testing motors and fixed gearboxes. There was not possibility of adding other components. Model of the test system is shown on Figure 25.

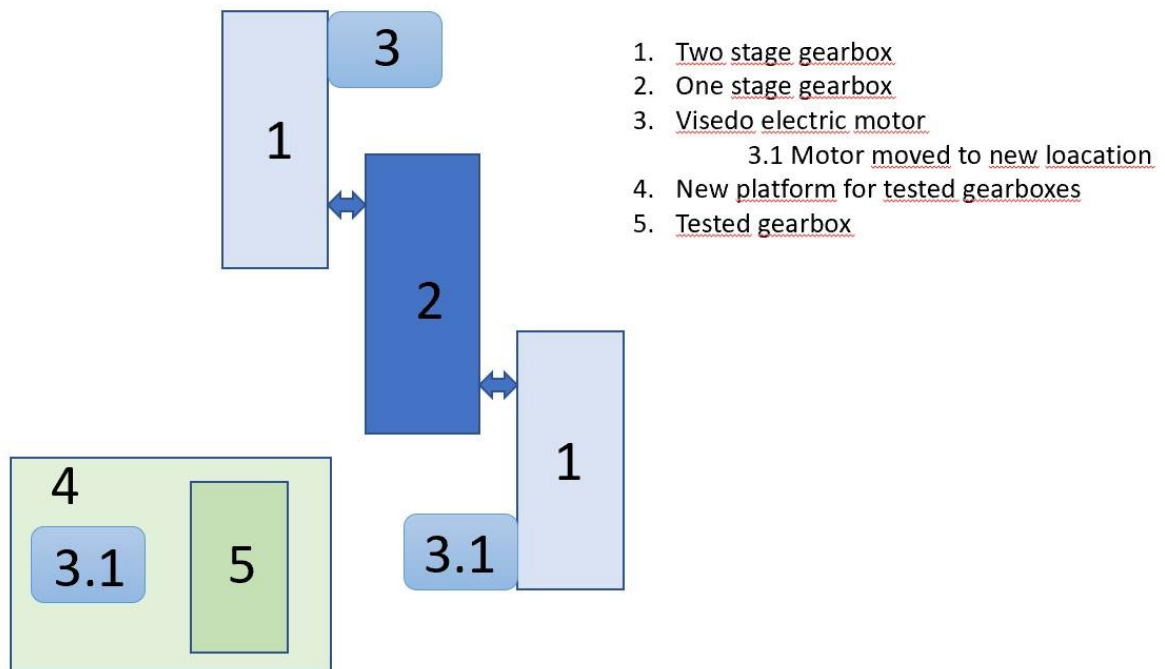


**Figure 25.** Schematic of test system layout

Plans to add side fixture for motor and tested gearboxes was started and some parts of it was already manufactured. Plans were not finished, and all installations needed to be designed. Work was started by sketching fixtures for tested gearboxes and measuring final place for frame in drawings. This was needed for mechanical install of frame and other components. Design work was done with larger team. Amount of work was too much for single person to do during thesis and because risks evolved needed peer review and verifications of design.

Cardan shaft to transfer power from test system to tested gearbox was acquired earlier. Basic frame for the tested gearbox was manufactured with several other smaller parts. It was clear that manufacturing and purchasing parts before finishing design process was limiting options. Altering existing parts was mandatory and caused loss of money and time. Structure wanted to be designed as modular as possible. Solution was to add smaller frames to the base frame.

Since objective was to design versatile solution, adjustability was taken into consideration. Aligning gearboxes with test system is crucial, selected cardan shaft allows maximum 5 degree of misalignment and target should be under two degrees.

### 3.6 Results of test bench design

Manufacturing tolerances of gearboxes and frames demanded adjustability of location of gearboxes. Measuring exact direction and location of tested gearbox from test system is quite challenging, so reference surface was added to basic frame so that alignment can be done with simple tools. This means that basic frame fastening to factory floor must be adjustable. This was executed by installing plate with adjusting screws to factory floor. (Figure 26) There were also uncertainties about the structure of the factory floor and it may be possible that fixtures cannot be placed exactly where desired.

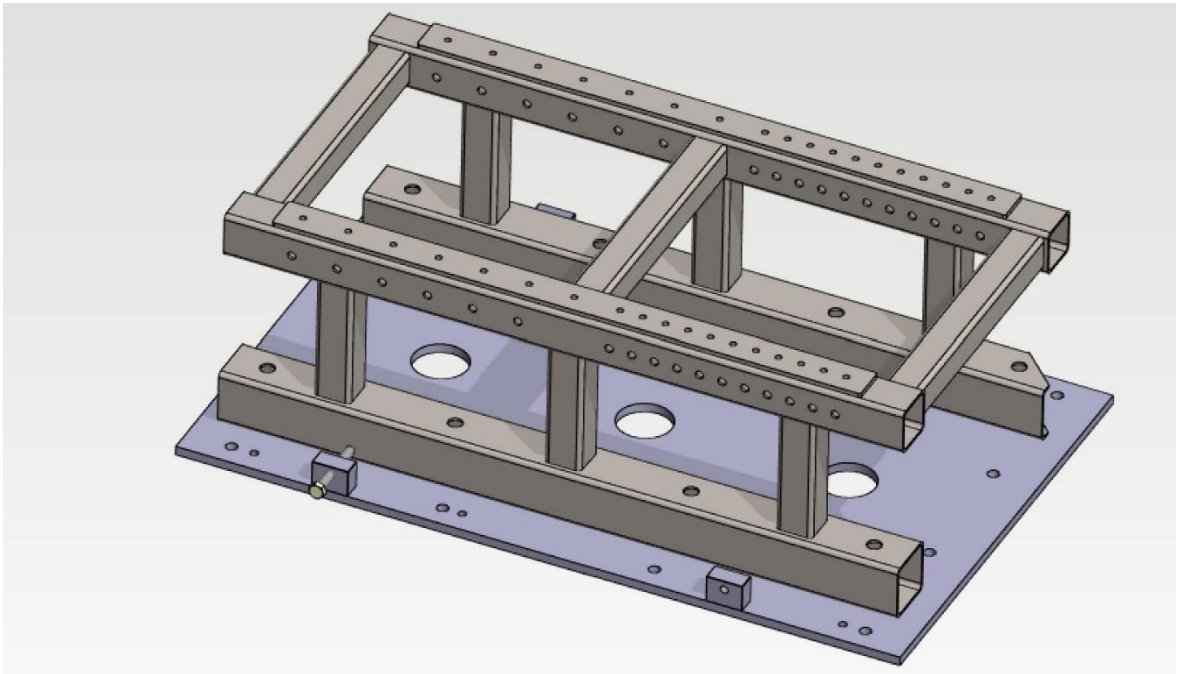


**Figure 26.** Basic frame with adjustable floorplate.

Both electric motors are capable of braking and accelerating. Gearboxes are controlled with two frequency converter each. This test is designed such way that motor attached to tested gearbox is braking and torque is delivered thru test system gearboxes.

Fast spinning heavy cardan causes high risks human to touch them or in failure, heavy and sharp fragments could fly quite far. Cardan shaft must be secured with protective case, showed in Figure 27. Sliding doors of the protection case are to provide access to flanges that connects gearbox and cardan shaft. Gearbox change is faster and safer when heavy shield can stay fixed in place.

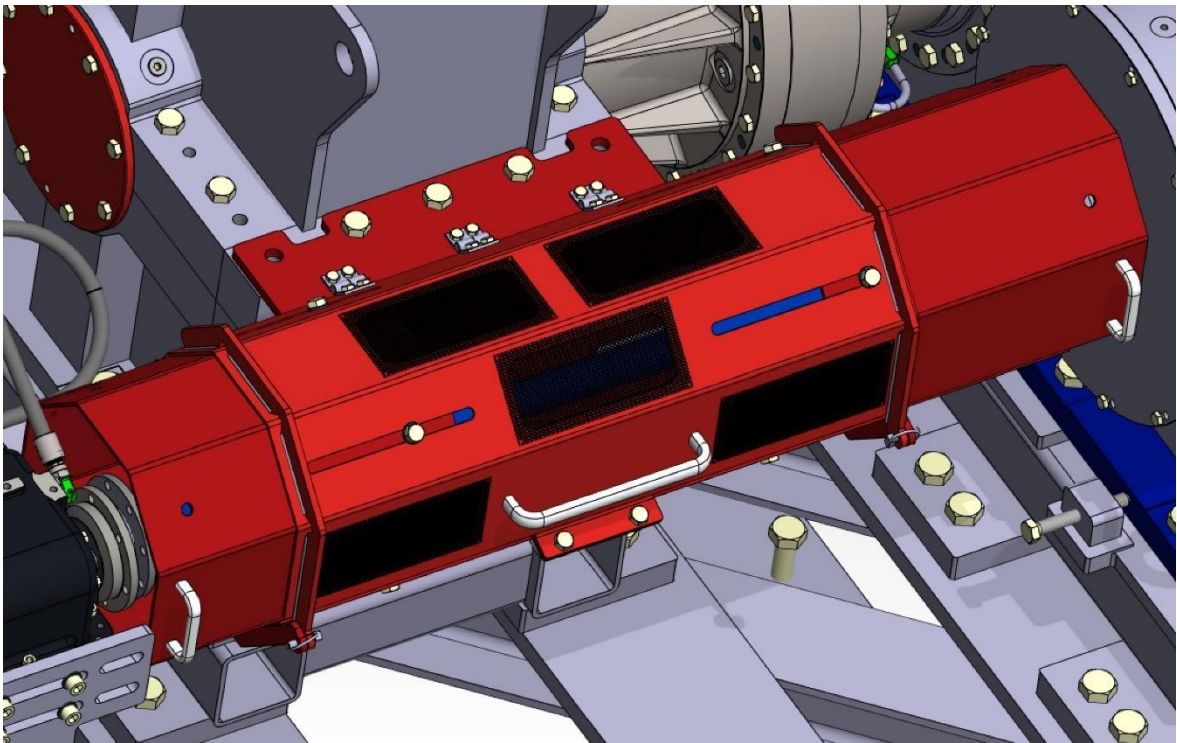


**Figure 27.** protective case to cardan shaft

These safety measures are considered enough now when the system is in development and all users are highly trained and understand all risks. It is preferable to install a fence around the whole test system before final introduction to production. Of course, proper risk evaluation and other mandatory requirements must be fulfilled before test is possible to begin. Actual production usage demands to fulfill CE-marking process.

Final design for test system is showing in Figure 28. Black gearbox is for the test designed in thesis. New design of test bench is modular and designed to accept parts from company other test systems if needed. Strong plate bolt in floor makes fine adjusting of frame possible. Frame is adjusted to specific location according to other parts of the test bench. This makes possible to use side of the frame as reference point when installing new devices. Motor or cardan shaft protection is not needed to remove when changing gearbox. Strength calculations were considered unnecessary since material selection and material thickness was exaggerated. This is quite a normal procedure when designing tools and fixtures in fixed multipurpose use. Added weight and cost is not critical in this kind of one time invest situations.

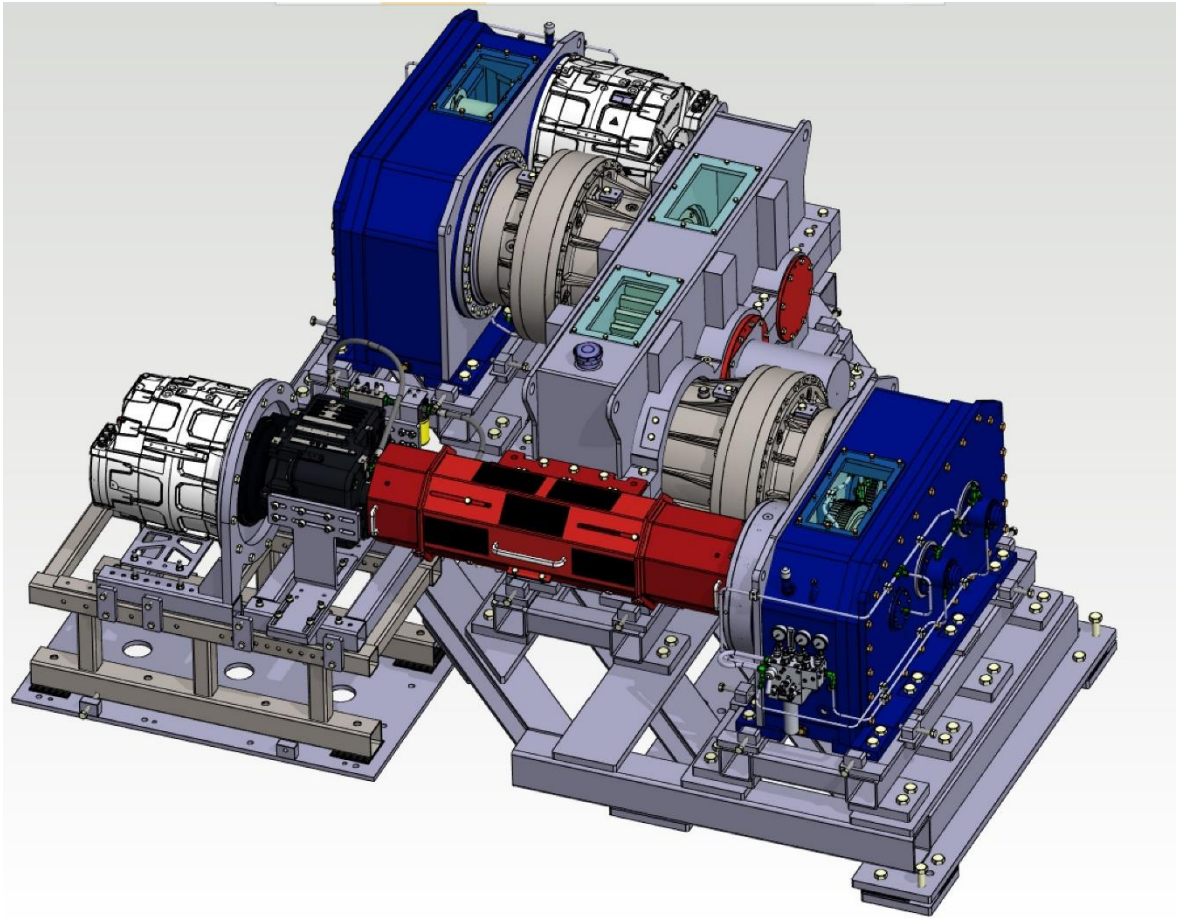


**Figure 28.** Model of the test system

Challenge in design process was to evaluate present and especially future needs. The structure was designed as modular as possible and to work also with existing equipment from other test systems used in the company.

## 4 CONCLUSION

Literature review showed that all factors are not included in calculations. This may produce some inaccuracies to gear strength calculation. Different materials are behaving differently in strength calculation as expected. However, it is not clear if this is just because of the different material strength and if the strength calculation takes note to different behavior in hardening process. This must be ensured by physical tests. A clearer difference was expected between calculations with different materials. KISSsoft expects base material hardness to be desired and not necessarily alert when hardness is too high. This needs to be verified with testing gearwheel strength and measuring hardness with destructive testing. Some parts of ISO 6336 standards are not mandatory but technical specifications. These parts give still important information to final results and should be taken into consideration in critical applications. Utilizing these newer calculations could result in more accurate strength calculations and thus make smaller and lighter gears possible. Also, full capability of KISSsoft FEM analysis is not utilized. Some added value could be found especially from tooth stress analysis.

Added section to test bench is now possible to manufacture and install. New part makes possible to test gearwheels from this thesis but also wide range of different gearboxes and other components which needed. Frame design makes possible to add almost any shape of fixture, with just maximum size limit. Most difficult part of this kind of design is to evaluate future needs. Everything is designed such a way that even yet unknown features are possible to add later when needed. Designing additional tests to ensure strength calculation accuracy from various aspects are possible and would be beneficial. More studies should be made to prove theories, concepts, and calculations. One of the most discussed topics with part customers is root shape of the gearwheel. Since shape of the root of the tooth is typically different than in the standard, there is often questions how it affects to final strength of the gearwheel. Results from test gears made with factory specific manufacturing methods, raw materials and calculations gives credibility and scientific proofing in discussions.



#### 4.1 Future studies

Next phase should be manufacturing gearwheels and make changes to test setup. Results of calculations should be verified by making test drives according to plan. All tests must be done in same way. Since safety factor and expected lifetime is short, all monitored factors and overall sound should be followed up closely all the time. If anomalies occur in sound from tested gears or from measured parameters gears should be checked out with endoscope.

Gear strength calculation have some room for improving in target company. All possible known aspects are not taken into consideration. The effect of gear strength calculation accuracy remains unknown. For example, ISO 6336-4, tooth flank fracture calculation, is not applied to calculation. Also, deeper analysis of tooth stress with KISSsoft FEM root stress module could give better understanding of existing reliability and safety levels. Since one goal of thesis was to find measures to improve gear strength calculation accuracy, logical recommendation is to add available additional calculations.

Test bench system needs still safety equipment and approval for them. Also, measure and probing abilities are almost endless. Test bench for gearwheel static strength would be beneficial to design. Static test gives accurate results since variables in test are limited to minimum. Strength calculation in KISSsys is easily made also to static load. This test is easy to design, and it should give another kind of verification of KISSsoft gear strength calculation accuracy on used materials and gear manufacturing methods. Dynamic test system for single gearwheel tooth could give important information from calculation accuracy in different situations. FZG tests should also be taken into consideration when improving calculation accuracy. Tests with bare gearwheels gives most accurate results of plain gearwheel strength calculation. Full-scale test like designed in thesis is quite difficult to interpret. It is not always possible to say which variable was causing the result and what change would be most effective. It could be possible to design attachment to test bench setup which makes static and dynamic loading of single gearwheel tooth possible. Accurately controlled and monitored motors with suitable lever action system could be simple attachment and gives more usability to system. Threshold to do single tests is much lower when test setup is in own control and does not need external equipment or labor.

## REFERENCES

Björling, M., Habchi, W., Bair, S., Larsson, R., Marklund, P., 2013. Towards the true prediction of EHL friction. *Tribology international*. [Online] 6619-26. p.10

Borremans, M., 2019. *Pumps and Compressors*. New York, N.Y: The American Society of Mechanical Engineers.p.481.

Concli, F., Fraccaroli, L., Maccioni, L., 2021a. Gear Root Bending Strength: A New Multiaxial Approach to Translate the Results of Single Tooth Bending Fatigue Tests to Meshing Gears. *Metals (Basel)* [Online] 11 (6), p.863.

Davis, J., 2005. *Gear materials, properties, and manufacture*. Materials Park. Ohio, ASM International. p.340.

Dennig, H.-J., Zumofen, L., Stierli, D., Kirchheim, A., Winterberg, S., 2021. Increasing the safety against scuffing of additive manufactured gear wheels by internal cooling channels. *Forchung im ingenieurwesen*. [Online] 63 (1), p.10.

DIN 6885-1., 2021. Drive type fastening without taper action, parallel keys, keyways – Deep pattern – Part 1: Dimensions, tolerances, mass. Berlin: Deutches Institute für Normung. DIN. p.24.

DNV-CG-0036., 2021. Calculation of gear rating for marine transmissions. DNV AS. p.90.

Gasparini, G., Mariani, U., Gorla, C., Filippini, M., Rosa, F., 2009. Bending Fatigue Tests of Helicopter Case Carburized Gears: Influence of Material Design and Manufacturing Parameters. *GearTechnology* 12, pp.68-76.

Goldfarb, V., Trubachev, E. & Barmina, N., 2020 *New Approaches to Gear Design and Production*. Volume 81. Springer International Publishing AG. p.529



Guillermo, E., Gabelli, A., 2019. Rolling bearing seizure and sliding effects on fatigue life. Proceedings of the Institution of Mechanical Engineers, Part J: Journal of Engineering Tribology, 233(2), pp.339-354.

Hansen, J., Björling, M., and Larsson, R., 2020. Lubricant film formation in rough surface non-conformal conjunctions subjected to GPa pressures and high slide-to-roll ratios. Scientific reports, 10(1), pp.1-16.

Hippenstiel, F., 2007. Tailored Solutions in Microalloyed Engineering Steels for the Power Transmission Industry. Materials Science Forum 539-543 Trans Tech Publications. Switzerland. pp.4131-4136.

Jelaska, D., 2012. Gears and Gear Drives. New York: John Wiley & Sons. p.437.

Kapelevich, A., Shekthman, Y., 2019. Optimization of asymmetric tooth root generated with protuberance hob. Gear solution, June. Pp.32-37.

Katsa. 2021 [Katsa webpage] Updated 2021. [Referred 27.10.2021]. Available: <https://www.katsa.fi/en/gearboxes-katsa/>

KISSsoft user manual., 2021. [web document]. (Publishing place unknown): KISSsoft, 2021. [Referred 22.11.2021]. Available: <https://www.kisssoft.com/en/products/technical-description>. p.943.

Kivivuori, S., 2016. Lämpökäsittelyoppi 2 – Lämpökäsittelytietoa suunnittelijoille. Helsinki. Teknologiateollisuus ry. p.320.

Maláková, S., Guzanová, A., Draganovská, D., Fedorko, G., Molnár, V., 2019. A case study of gear wheel material and heat treatment effect on gearbox strength calculation. Journal of Mechanical Science and Technology, 33(12), pp.5817-5827.

Nutakor, C., Klodowski, A., Sopenan, J., Mikkola, A., Pedrero, J., 2017. Planetary gear sets power loss modeling: Application to wind turbines. *Tribology international*. [Online] 10542-54. p.13.

Nutakor, C., Talbot, D., Kahraman, A., 2019. An experimental characterization of the friction of a wind turbine gearbox lubricant. *Wind energy*. Chichester, England. [Online] 22 (4), Pp.509-522.

P90G., 2021. [Gleason webpage]. [Referred 29.11.2021]. Available: <https://www.gleason.com/en/products/machines/cylindrical/profile-grinding/p90g-the-universal-solution-for-smaller-gears>

Ramasamy, R., Durairaj, S., Ganesan, T., Rao, P., 2020. Reliability Design for Bending Fatigue Strength of Carburized Gears of Low-Carbon Case Hardenable Steels 20CrMo, 20MnCr5, and SAE 8620. *Advances in Lightweight Materials and Structures*. [Online]. Singapore: Springer Singapore. pp.521–529.

Rycerz, P., and Kadiric, A., 2019. The influence of slide–roll ratio on the extent of micropitting damage in rolling–sliding contacts pertinent to gear applications. *Tribology Letters*, 67(2), p.63.

Semken, R., Nutakor, C., Mikkola, A. and Alexandrova, Y., 2015. Lightweight stator structure for a large diameter direct - drive permanent magnet synchronous generator intended for wind turbines. *IET Renewable Power Generation*, 9(7), pp.711-719.

SFS-ISO 1328-1., 2016. Cylindrical gears – ISO system of flank tolerance classification – Part 1: Definitions and allowable values of deviations relevant to flanks of gear teeth. Helsinki: Suomen Standardoimisliitto SFS. p.51. Confirmed and published in English.

SFS-ISO 53., 2012. Cylindrical gears for general and heavy engineering- Standard basic rack tooth profile. Helsinki: Suomen Standardoimisliitto SFS. p.12. Confirmed and published in English.

SFS-ISO 6336-1., 2020 Calculation of load capacity of spur and helical gears – Part 1: Basic principles, introduction and general influence factors. Helsinki: Suomen Standardoimisliitto SFS. p.140. Confirmed and published in English.

SFS-ISO 6336-2., 2020 Calculation of load capacity of spur and helical gears – Part 2: Calculation of surface durability (pitting). Helsinki: Suomen Standardoimisliitto SFS. p.43. Confirmed and published in English.

SFS-ISO 6336-3., 2020 Calculation of load capacity of spur and helical gears – Part 3: Calculation of tooth bending strength. Helsinki: Suomen Standardoimisliitto SFS. p.62. Confirmed and published in English.

SFS-ISO 6336-4., 2020 Calculation of load capacity of spur and helical gears – Part 4: Calculation of tooth flank fracture load capacity. Helsinki: Suomen Standardoimisliitto SFS. p.29. Confirmed and published in English.

Terrin, A., Meneghetti, G., 2018. A comparison of rolling contact fatigue behaviour of 17NiCrMo6-4 case-hardened disc specimens and gears. In: *Fatigue & Fracture of Engineering Materials & Structures: Special issue: Manufacturing influence on Fatigue Properties*. John Wiley & Sons, Ltd. Pp.2321-2337.

Tobie, T., Hippenstiel, F., Mohrbracher, H., 2017. Optimizing Gear Performance by Alloy Modification of Carburizing Steels. *Metals* 7(10) 415. p.20

Vullo, V., 2020a. *Gears: Volume 1: Geometric and Kinematic Design*. Springer International Publishing AG. p.844.

Vullo, V., 2020b. *Gears: Volume 2: Analysis of Load Carrying Capacity and Strength Design*. Springer International Publishing AG. p.623.







Drawing of gearwheel two 20MnCr5

